GENERATING PLANT LINES WITH MARKERS DESIGNED TO ASSESS CELL POLARITY DEFECTS AT THE MOLECULAR LEVEL

UTSAB PAGENI
BACHELOR IN AGRICULTURAL SCIENCE, TRIBHUVAN UNIVERSITY, 2016

A thesis submitted
in partial fulfilment of the requirements for the degree of

MASTER OF SCIENCE

In

BIOLOGICAL SCIENCES

University of Lethbridge
LETHBRIDGE, ALBERTA, CANADA

GENERATING PLANT LINES WITH MARKERS DESIGNED TO ASSESS CELL POLARITY DEFECTS AT MOLECULAR LEVEL

UTSAB PAGENI

Date of Defense: July 14, 2021

Dr. E. Schultz Supervisor	Associate Professor, Ph.D.
Dr. R. Golsteyn Thesis Examination Committee Member	Associate Professor, Ph.D.
Dr. T. Russell Thesis Examination Committee Member	Associate Professor, Ph.D.
Dr. R. Laird Chair, Thesis Examination Committee	Associate Professor, Ph.D.

Dedication

To my beloved grandparents

Abstract

Cellular polarity is a fundamental aspect of all multicellular organisms that enables certain cell types to carry out their functions. Therefore, cell polarity formation is an important basis for understanding the molecular linkage between morphology and cellular functions. In *Arabidopsis*, the position of root hairs is mediated by intercellular flow of the phytohormone auxin, for which directional signaling is determined by the polar subcellular localization of PIN-FORMED (PIN) transport proteins. My research primarily focuses on establishing plant lines that will later allow correlation of changes in proteins distribution with changes in cell polarity and plant morphology. Mutations in genes such as *FORKED1*, *SCARFACE, PINOID* and *RON3* result in defective localization of PIN proteins in various tissues, by affecting PIN phosphorylation status (PID and RON3) or endomembrane dynamics (FORKED1 and SCARFACE). This study will introduce fluorophore labeled fusion proteins into *FORKED1*, *SCARFACE, PINOID* and *RON3* mutants.

ACKNOWLEDGMENTS

I am very grateful for my thesis supervisor, Dr. Elizabeth Schultz, for her consistent support, enormous contribution, and patience throughout my program. I am thankful to her for providing me an opportunity to study abroad and going above and beyond in helping me complete my thesis. I would like to thank my supervisory committee members, Dr. Roy Golsteyn and Dr. Tony Russell for their valuable comments, suggestions, and encouragement. At this moment of time, I am thankful to Schultz lab members, Kurt, Jaxon, Leanne, and my peers at the University of Lethbridge for always being cooperative and supportive. A big thanks to Maurice for helping me gain more technical skills and training me on the confocal microscope. I am very thankful to the University of Lethbridge and all supportive departments, NSERC for providing me with a great working environment and financial support. Thank you to my parents for their unconditional love and encouragement. An immense thank you to my family in Canada for helping me adjust to life in Canada and their constant support throughout my graduate degree. Finally, I would like to express my gratitude to everyone out there who helped me in one way or another during my degree.

TABLE OF CONTENTS

List of Tables

LIST OF FIGURES

LIST OF ANNOTATIONS, ABBREVIATIONS AND GENE SYNONYMS

Annotations

FORKED1 – wild type gene is capitalized and italicized
forked1 – mutant gene is italicized
FORKED1 – protein is capitalized

Abbreviations

ABRC = Arabidopsis Biological Resource Centre
ABCB = ATP-BINDING CASSETTE SUBFAMILY B
ARF = ADP RIBOSYLATION FACTOR
AUX1/LAX = AUXIN RESISTANT1/LIKE AUX1
BFA = Brefeldin A
BIG = BREFELDIN A INHIBITED ARF GUANINE EXCHANGE FACTOR
CHCL3 = Chloroform
COP I = COAT PROTEIN COMPLEX
CVL1 = COTYLEDON VASCULAR PATTERN 2 LIKE1
CVP2 = COTYLEDON VASCULAR PATTERN 2
DAG = Days After Germination
DNA = Deoxyribonucleic acid
D6PK = D6 Protein Kinase
DUF828 = Domain of Unknown function
EZ = Elongation Zone
FL = FORKED1-LIKE
FKD1 = FORKED1
FKD2 = FORKED2
GA = Golgi Apparatus
GAP = GTPASE-ACTIVATING PROTEIN
GEF = GUANINE NUCLEOTIDE EXCHANGE FACTOR
GFP = Green Fluorescent Protein
GNL1= GNOM LIKE 1
GNL 2 = GNOM LIKE 2
GUS = β-Glucuronidase
IAA = Indole 3-Acetic Acid
LB = Left Border
MZ = Meristematic Zone
NAA = 1-Naphthaleneacetic Acid
PA = Phosphatidic Acid
PGR = Plant Growth Regulators
PGP = P-GLYCOPROTEINS
PH = Pleckstrin Homology
PI = Phosphoinositides
PM = Plasma Membrane
PI (4)P = Phosphatidylinositol-4 monophosphate
PIN = PINFORMED
PID = PINOID
PP2A = PROTEIN PHOSPHATASE 2
QC = Quiescent Centre

RFP = Red Fluorescent Protein
rhd6 = root hair defective6
SAM = Shoot Apical Meristem
S.D = Standard Deviation
SFC = SCARFACE
SYP = SYNTAXIN OF PLANTS
TAA = TRYPTOPHAN AMINOTRANFERASE OF ARABIDOPSIS
TBE = Tris/Borate/EDTA
T-DNA = Transfer-DNA
TGN = Trans Golgi Network
VAN3 = VASCULAR NETWORK DEFECTIVE 3
VI = Vascular Island
WT = Wild Type
YFP = Yellow Fluorescent Protein
YUC = YUCCA

Gene synonyms

BIG5 = BEN1 = MIN7
FKD2 = SFC = VAN3

Chapter 1: Literature Review

1. Auxin

1.1 Introduction to Auxin:

Plant growth regulators (PGRs) are chemical hormones that have a significant effect on the overall growth and development of plants. Indole 3-Acetic Acid (IAA) was the first plant hormone to be discovered. It is the predominant auxin found in plants and has been recognized as the major auxin for more than 70 years. Auxin and its role in plant growth was first experimentally demonstrated in plants in 1928 by Dutch biologist Frits Warmolt Went. Auxin is derived from the Greek word aux-ein, which means increase in growth. Auxin is an indispensable hormone with multiple functions in different aspects of growth and development including cell expansion and differentiation (Fukuda, 2004), organogenesis and tropisms (Weijers et al., 2006) and apical dominance (Reed, 2001). Such developmental processes are influenced by the local accumulation and depletion of auxin (Mockaitis and Estelle, 2008)

1.2 Synthesis of auxin.

Most auxin is synthesized in the shoot apex and young leaves, thus auxin transport from the sites of synthesis (source tissue), such as shoots, to the sites of action (sink tissue), such as roots, is very important for plant development (Ljung et al., 2001). Earlier research indicated that auxin synthesis was limited to aerial parts like young shoots and immature leaves (Ljung et al., 2001) but later research demonstrated that auxin biosynthesis also happens in meristematic tissues within the primary root and at the tips of lateral roots (Ljung et al., 2005). Auxin is synthesized by both tryptophan dependent and independent pathways. In the tryptophan dependent pathway, tryptophan

is a major precursor for synthesis of IAA (Zhao, 2012). In *Arabidopsis*, the enzymes TRYPTOPHAN AMINOTRANSFERASE of *Arabidopsis* (TAA), which produces indole 3-pyruvic acid (IPA) from tryptophan, and YUCCA (YUC) flavin monooxygenase-like proteins, which produce IAA from IPA, are sequentially required for biosynthesis of IAA from tryptophan during plant development (Mashiguchi et al., 2011). The transport of auxin from regions of biosynthesis to low concentration areas, or sink tissues, is crucial for the establishment of auxin gradients and the disruption of these gradients can induce many auxin-related developmental defects (Swarup and Péret, 2012).

1.3 Model of auxin transport

The chemiosmotic model of auxin transport involves efflux and influx carriers as auxin is a weak acid and its ability to cross the plasma membrane is dependent on pH. Transport of auxin involves either long-distance transport through mature phloem, which is used to transport auxin from young shoot (source) to root (sink) tissues (Petrášek and Friml, 2009) or short-range transport in a cell-to-cell manner, which is dependent on specific auxin carriers (Peer et al., 2011). Polar auxin transport (PAT) involves auxin influx and efflux carrier proteins and leads to establishment of auxin gradients (Vieten et al., 2005; Chandler, 2009). Auxin can enter the cell either by passive diffusion of the protonated form (IAAH) across the cell membrane or by transport of the anionic or unprotonated form (IAA^-) via auxin influx carrier proteins. The slightly acidic extracellular environment (pH 5.5), favours undissociated IAA, which will pass through the membrane via passive diffusion into cytosol. After auxin (IAAH) enters the cells, the cytosol pH is more alkaline, promoting dissociation into IAA^- and H^+ (Robert and Friml, 2009). IAA^- is unable to leave the cell without the action of efflux carriers. This pH dependent dynamic equilibrium means that PAT is absolutely dependent on efflux carriers, but less influenced by influx carriers. Efflux and influx

occur through the action of three protein families: AUXIN RESISTANT 1/LIKE AUX1 (AUX/LAX) encode the major influx carriers, while the PIN-FORMED (PIN) and the ABCB/PGP (ATP-BINDING CASSETTE SUBFAMILY B/P-GLYCOPROTEINS) encode the major auxin efflux transporters (Péret et al., 2012). The best-characterized transporters of the ABCB/PGP group are ABCB1/PGP1 (found in all root cells except the columella cells), ABCB4/PGP4 and ABCB19/PGP19 (only in endodermis and pericycle) (Overvoorde et al., 2010). Since their location in the plasma membrane is mostly non-polar, ABCB/PGP transporters mediate non-directional auxin efflux and are likely to be important both for long-distance auxin transport and for local auxin gradient and auxin maxima/minima formation (Zažímalová et al., 2010). PIN proteins act as efflux carriers for auxin throughout the plant tissues and organs. In *Arabidopsis thaliana*, the PIN protein family consist of eight members (PIN1-PIN8). PIN proteins are classified into two groups: long PINs, including PIN1, 2, 3, 4 and 7, are the major auxin efflux carriers and exhibit plasma membrane (PM) localization (Petrášek et al., 2006); short PINs, including PIN 5, 6 and 8, are localized to the endoplasmic reticulum and are involved in homeostatic auxin compartmentalization (Mravec et al., 2009). Fluorescently labeled protein expression and transcription profiling illustrate that PIN1, 3, 4, and 7 are expressed globally during development, but exhibit tissue-specific expression intensity and polarity (Vieten et al., 2005). Localization of the long PINs, PIN1, 2, 3, 4 and 7, to the plasma membrane in different cell types confers directional auxin transport within different tissues. Localization of PIN proteins to the apical face of the plasma membrane leads to upward auxin transport, whereas the basal localization of PIN proteins leads to downward auxin transport (Adamowski and Friml, 2015).

By controlling formation of auxin gradients, functions of PIN proteins include root meristem maintenance (PIN1, 3, 4 and 7) (Peer et al., 2011) and vascular tissue differentiation and

regeneration (PIN1, 5, 6, and 8) (Sawchuk and Scarpella, 2013). Because asymmetric subcellular localization of PIN proteins has primarily been found to determine directionality of auxin flow, my focus in the next sections will be on PIN proteins and how they control polarity during plant development.

1.4 Cellular polarity

A cell can be described as having polarity when aspects of its development or function occur preferentially in one axis or one direction. Cell polarity has an essential role in all cellular organisms as the polarity of cells at an individual level predetermines how the cells will grow, divide mitotically, and create mature tissue (Shao and Dong, 2016). At the cellular level in animals, cell polarity is understood to play roles in processes including gastrulation, neural development and organ tissue generation (Gray et al., 2011). During morphogenesis, the directionality created by the asymmetrical distribution of cellular components may generate new axes of polarity which signal the differentiation of complex structures (Cove, 2000). In plant cells, the asymmetric localization of PIN proteins which distribute auxin are an example of cellular polarity which is thought to influence tissue morphology.

Planar cell polarity is the polarization of cells within the plane of a cell sheet. Two examples of planar cell polarity in plants are the polarization of root hair emergence from root epidermal cells (trichoblasts) along the apical-basal axis (Fischer et al., 2007) and the polarization of epidermal cells along the proximal-distal leaf axis which is thought to impact leaf morphology (Kuchen et al., 2012). Interference with auxin transport alters the root hair position (Fischer et al., 2007). These experiments provide strong evidence that in the root epidermis, planar polarity is controlled by PIN regulated auxin transport. In the leaf epidermis, the polarity of one cell has been shown to influence surrounding cells and tissues thus creating cell polarity and impacting leaf

morphology; modeling experiments show that control of polarity of leaf epidermal cells by PIN1 would be consistent with this influence (Kuchen et al., 2012). These studies have led to the idea that the establishment of planar cell polarity in root or leaf tissue relies on the asymmetric distribution pattern of the phytohormone auxin.

1.5 Root development

Roots allow the plant to uptake water and nutrients to thrive in its environment (Petricka, Winter, and Benfey, 2012). The development of roots in *Arabidopsis* involves different steps. The root is generated throughout plant growth by the root apical meristem, which is established early in embryogenesis. The primary root emerges from the seed upon germination and grows gravitropically into the soil by cell division in the meristematic zone and subsequent cell elongation in the elongation zone (Beemster and Baskin, 1998). In general, the root system maintains at least two types of roots: the primary root, which forms directly from divisions within the root apical meristem and lateral roots, which are initiated post-embryonically from cell divisions within the pericycle of primary roots (Celenza et al., 1995). Also, certain plants can develop adventitious roots, which emerge from non-root tissues, such as stems and leaves (Verstraeten, Schotte, and Geelen, 2014).

1.5.1 Developmental zones of the root

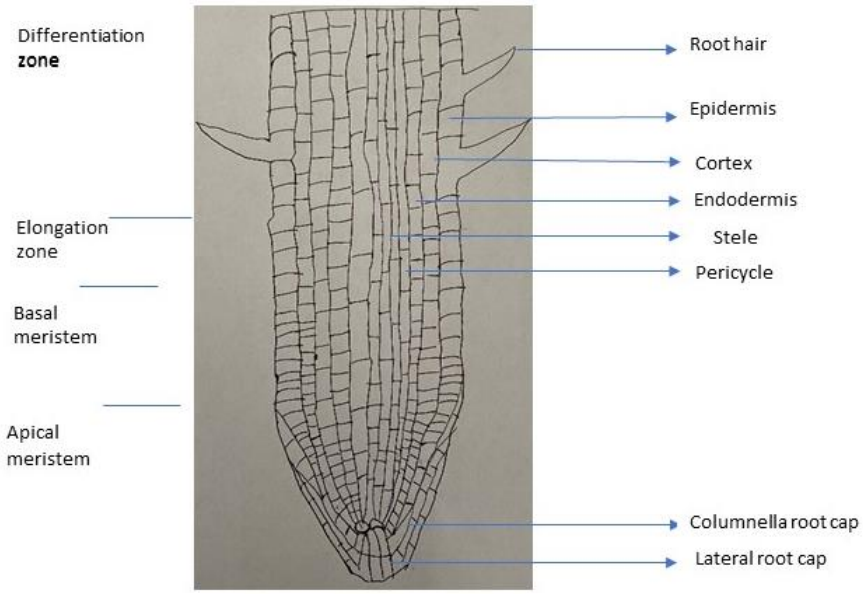

Figure 1: Organization of Arabidopsis root showing different zones and cells

Newly formed cells in the root apical meristem (RAM) progress through three different zones (*Figure 1*): i) Zone of cell division or stem cell zone is close to the root tip and is composed of dividing cells of root meristem. The meristematic zone is categorized into basal and apical meristems. Cell division occurs in both the apical meristem and the basal meristem. The basal meristem is also called the transition domain. Newly formed cells in the RAM divide for 4-6 cycles in the basal meristem, where cell division occurs both anticlinally, to increase root length, and periclinally, to increase root girth and generate additional tissue fates, such as the cortex and endodermal regions. ii) The zone of elongation (EZ) contains nascent cells that increase in length; older proliferating cells move from the stem-cell niche into the elongation zone; iii) zone of cell maturation (MZ) is where root cells differentiate into specialized cell types, such as trichoblasts bearing root hairs, and acquire final length.

1.5.2 Polar auxin transport within the root.

The different zones within the root meristem are controlled in part by auxin levels established by PAT. Auxin is first transported to the RAM from the shoot and is then laterally redistributed at the columella and transported shootward through the root epidermis. This "reverse fountain effect" is controlled by 5 different PIN family members differentially expressed in the different root cell types. Through the action of basally localized PIN1, PIN3 and PIN7 in the vascular parenchyma, phloem and endodermal cells, auxin is initially transported from the shoot to the meristematic zone of the RAM. PIN1 localizes at the basal plasma membrane of the stele and endodermal cells and directs auxin transport towards the root meristem (Friml et al., 2002). *PIN2, PIN3* and *PIN4* are mainly expressed in the areas of cell division and elongation and control the auxin maximum and auxin redistribution in the columella (Friml et al., 2002). PIN2 is basally localized in cortical cells, which contributes to auxin transport towards the root tip, while its apical localization in root epidermal cells and root cap contributes to auxin transport towards the shoot (Friml et al., 2003). In the elongation zone of roots, PIN3 is localized to the lateral membrane of pericycle cells where it controls the lateral movement of auxin (Keuskamp et al., 2010). In root columella cells, PIN3 is equally distributed throughout the plasma membrane and re-localizes laterally on gravity stimulation (Friml et al., 2002). PIN4 localizes to the basal PM in vascular cells and is expressed in the quiescent center and in columella cells where it mediates auxin flow and redistribution for root elongation and gravitropism (Friml et al., 2002). The apical localization of PIN2 in root epidermal cells and the lateral root cap contributes to auxin transport towards the shoot (Friml et al., 2003).

The reverse fountain of auxin movement within the root tip generates auxin levels that are higher in the meristematic zone than in the elongation zone, and maintenance of an auxin balance

is important to coordinate developmental processes (Kong et al., 2018). The auxin maintenance in meristematic and elongation zone is mainly achieved by both root-ward transport through basal membrane localized PIN1 and PIN7 (pro-vascular cells), PIN2 (cortical cells) and PIN3 (vascular cells), and shoot-ward transport through apically localized PIN2 (epidermal cells) between meristematic zone and elongation zone (Vieten et al., 2005; Keuskamp et al., 2010; Adamowski and Friml, 2015). The bending of roots towards gravity also depends on auxin distribution. Redistribution of auxin in gravistimulated roots has been shown to be dependent upon the action of AUX1 and PIN2 protein in both epidermal and lateral root cap cells (Swarup et al., 2005). Auxin redistribution results in increased auxin levels on one side of the root epidermis than the other, causing root bending (Swarup et al., 2005).

1.5.3 Emergence of root hair from trichoblast shows polarity.

The absorptive surface area of roots is greatly increased through the production of epidermal cell projections known as root hairs. Epidermal cells of roots which form root hairs are known as trichoblasts (Dolan et al., 1993). Initiation of a root hair on the outer surface of a trichoblast appears as a bulge due to localized loosening of cell wall. In *Arabidopsis*, the shifting position of root hair emergence on the trichoblast is the prime system for studying cellular polarity and cellular organisation (Fischer et al., 2007). Mutation to the auxin influx carrier AUX1 causes reduced auxin levels in the root tip because of impaired basipetal auxin transport (Swarup et al., 2005). *aux1* loss-of-function mutants display weak apical shifts of hair position and occasional formation of two hairs per trichoblast, suggesting that AUX1 is one component of the auxin transport machinery which regulates planar polarity of hair positioning in *Arabidopsis* (Fischer et al., 2007). In the experiment by Fischer in 2007, *root hair defective 6* (*rhd6)* mutants were found to have upward and downward shift in root hairs, which were normalized by application of auxin.

1.6 Role of auxin in leaf morphology development

Auxin plays a significant role in the development of the leaf, as it regulates cell division and elongation. PIN1 is the major non-redundant member of the family involved in shoot development; it is expressed in apical parts of early embryos, throughout the vascular tissues, in the shoot apical meristem and in developing primordia (Gälweiler et al., 1998). PIN3 localizes laterally at the inner side of stem endodermal cells (Grunewald and Friml, 2010) and is important in controlling the stem response to gravity and light. PIN5 is expressed in hypocotyl, cauline leaves and guard cells of stomata (Mravec et al., 2009).

1.6.1 Leaf primordia initiation and phyllotaxis

The growth region of the plant shoot, the shoot apical meristem (SAM), contains pluripotent stem cells that develop for the formation of new organ primordia and give rise to all the tissue of the shoot. The development of leaves starts from initiation of leaf primordia that occur at a region of high auxin concentration in the shoot apical meristem. In the first step, because PIN1 is localized to the apical side of epidermal cells, auxin is transported through the epidermis from both sides of the SAM, which results in formation of an auxin convergence point (Reinhardt et al., 2003). The auxin maximum at the convergence point defines the primordium. During the second step, the positive correlation between auxin and its efflux transporter PIN1 activates *PIN1* expression in the ground tissue underlying the epidermis. In the ground tissue, the PIN1 is basally localized within a narrow canal of cells based on the principle of auxin canalization, which causes auxin transport into the future midvein (Benková et al., 2003). The movement of auxin into the ground tissue means that auxin is depleted from the SAM, defining an exclusion zone around the primordium where no other primordia can form.

1.6.2 Leaf development

The development of a leaf from its origin as a small primordium to a mature leaf occurs via growth and differentiation along three different developmental axes, the abaxial-adaxial (also called dorsoventral), whose orientation is in the up-down direction, the medio-lateral (also called centro-lateral), which orients middle to side direction and thirdly, the proximo-distal which has longitudinal orientation. The adaxial–abaxial (top-bottom) axis of asymmetry involves specialization of the upper and lower leaf surfaces. Leaf mesophyll is ground tissue which is internal whereas stomata are within the epidermal tissue. All three tissue layers (epidermal, ground and stele) are polarized along abaxial-adaxial sides. In the epidermis, trichomes form more frequently on the adaxial side, whereas more stomata form on the abaxial side. Within the stele, xylem is formed towards the adaxial and phloem toward the abaxial. Within the ground tissue, palisade mesophyll forms towards the adaxial while spongy mesophyll forms on the abaxial side. Leaf margins are formed at the boundary of the adaxial and abaxial domains and the extension of the lamina results from adaxial–abaxial patterning of the developing primordium. The leaf proximodistal axis defines growth of the leaf away from the stem and later establishment of distinct proximal and distal cells which develop into leaf petiole and the leaf blade (Ichihashi and Tsukaya, 2015). Auxin plays an important role in coordinating proximodistal and adaxial-abaxial axes beyond leaf initiation stages, for example, it has been found that accumulation of auxin is more at the distal part of leaf and in developing vasculature (Reinhardt et al., 2000).

1.6.3 Establishment of leaf venation and PIN1 localization in leaves

Leaf venation and its modifications play important roles in plant productivity by influencing photosynthesis and plant survival in response to environmental conditions (de Boer et al., 2016). The typical hierarchal, reticulate pattern of angiosperm venation has been a major advantage in

angiosperm productivity over other plants (de Boer et al., 2016). To adapt to arid environments, angiosperms have evolved higher levels of major vein density (Sack and Scoffoni, 2013). The increase in major vein density may be due to preference for smaller, thicker, and longer-lived leaves in arid environments that are transiently exposed to water (Gorai et al., 2015). By having higher major vein density, plants transiently exposed to increased water availability can have temporarily high photosynthetic rates and maintain efficient water transport to the thicker mesophyll tissues reducing desiccation (de Boer et al., 2016).

As described above, the localization of PIN1 in the epidermis of the leaf primordium initiates PIN1 expression in the ground tissue that will become the midvein; the process is reiterated to initiate secondary veins (Scarpella et al., 2006). PIN1 expression is turned on in ground cell layers beneath the convergence points in a triangular expression domain (Hou et al.,2010; Scarpella et al., 2006; Mariyamma et al., 2018). Within the outside cells of the expression domains that predict midvein and secondary vein position, PIN1 polarizes laterally towards the inner cells thereby concentrating auxin from surrounding areas and focusing the mid vein to narrow file of cells (Bayer et al., 2009; Mariyamma et al., 2018). Thus, polarization of PIN protein localization results in the canalization of auxin transport into a subset of cells; the resulting high auxin concentration causes cells to adopt a vascular fate (Sauer et al., 2006). The formation of secondary veins in *Arabidopsis* occurs in two stages, the first being the formation of the lower loop domain and the second the formation of the upper loop domain (Scarpella et al., 2006). After the establishing the auxin convergence point that defines the midvein, PIN1 proteins within epidermal cells in the distal margin of the leaf shift their localization from apical to basal thereby directing auxin flow downwards in the leaf margin and a creating convergence point on each side of leaf (Scarpella et al., 2006). In a similar fashion to the definition of the midvein, these convergence

points define the position of secondary veins and initiate the formation of the lower loop domain. PIN1 expression and basal localization extends within the ground tissue towards the midvein, forming a connection. Next, expression of PIN1 is initiated in the upper loop domain, which extends towards the distal midvein producing a continuous secondary vein connected to the midvein at two points (Scarpella et al., 2006). The connection of each upper loop domain and lower loop domain requires a single bi-polar cell with both apically and basally localized PIN1 (Scarpella et al., 2006).

1.7 Endomembrane system and vesicle transport

The directed transport of proteins like PIN to the plasma membrane (PM), which, as described above, is important to PAT and thus many aspects of plant development, involves a complex endomembrane system consisting of membrane enclosed organelles such as endoplasmic reticulum (ER), Golgi apparatus (GA), trans-Golgi network (TGN), lysosomes, endosomes and vacuoles, each of which contains a unique membrane composition and cargo proteins (Bonifacino and Glick, 2004). There are three different pathways involved in transport of PM localized proteins: secretory, endocytic and retrieval pathways (Bonifacino and Glick, 2004). The secretory pathway is involved in secretion of vesicles from the endoplasmic reticulum (ER) to the plasma membrane (PM), whereas endocytosis is involved in recycling of vesicles from the PM to late lysosomes. The secretory pathway involves protein transport to PM via ER and GA (Jürgens, 2004). Endocytosis includes recycling of PM proteins via early endosomes, and late endosomes are involved in GA to vacuole trafficking or traffic directly from TGN to late endosomes (Jürgens, 2004). In plants, endocytic and secretory pathways have been found to merge within the TGN (Viotti et al., 2010, because proteins that mark the endosomes, such as SYNTAXIN OF PLANTS61 (SYP61), can label both TGN and EE (Drakakaki et al., 2012).

1.8 Phosphoinositides involved in PIN localization

Phosphoinositides are involved in endomembrane trafficking by regulating localization of proteins like PIN1 to control cell polarities, for example during tip growth of root hairs and pollen tubes (Tejos et al., 2014). Phosphoinositides (PIs) are membrane phospholipids with a phosphorylated inositol head that exist in all tissues and cell types (Heilmann, 2016). They are precursors of various secondary messengers, can activate many enzymes and are also involved in trafficking of proteins to the plasma membrane (Heilmann, 2016). One domain which contributes to protein localization via an interaction with PIs is the Pleckstrin Homology (PH) domain (Wakelam and Lemmon, 2007). There are many PIs found in plants which are at very precise locations. PI3P and PI (3,5) P2, which are found in the late endosomes and vacuoles, regulate endomembrane trafficking in the context of autophagy and are important for vacuolar/tonoplast functions (Heilmann, 2016). The phosphoinositides PI4P and PI (4,5) P2 have a role in PIN1 transport to the root epidermal membrane (Tejos et al., 2014), PI (4,5) P2 mainly exists on the PM and a gradient of PI4P has been confirmed, with the highest amount at the PM, an intermediate amount in post-Golgi/endosomal compartments, and the lowest amount in the GA (Simon et al., 2014).

1.8.1 *COTYLEDON VASCULAR PATTERN 2 (CVP2)*

Mutations that affect PI distribution and abundance affect PIN localization and result in auxin transport dependent phenotypes. For example, *COTYLEDON VASCULAR PATTERN 2* (*CVP2*) encodes an inositol polyphosphate 5’ phosphatase that catalyzes the switch from PI (4,5) P2 to PI4P, and mutation in *CVP2* results in leaves with discontinuous veins (Carland and Nelson, 2004) *CVP2 LIKE 1* (*CVL1*) is the closest homolog to *CVP2*, and mutation in both genes results in lower PI4P yield, shorter root growth with more dense lateral roots, and more severe cotyledon and

leaf vasculature defects, which suggests functional redundancy (Carland and Nelson, 2009; Naramoto et al., 2009; Rodriguez-Villalon 2015). Regulation of phosphoinositide levels by *CVP2* and *CVL1* has been proposed to affect auxin flow by PIN1 regulation (Naramoto et al., 2009).

1.8.2 Involvement of coat proteins and G proteins in vesicle transport

The endomembrane trafficking system mediating transport of vesicles is controlled by many factors such as coat proteins, dynamin, SNAREs and G-proteins. Dynamin is a GTPase that plays a vital role in clathrin-dependent endocytosis and other vesicular trafficking processes by acting as a pair of molecular scissors for newly formed vesicles originating from the plasma membrane (Singh et al., 2017). SNARE proteins catalyze the membrane fusion reactions in vesicle transport. There are two type of SNAREs proteins: vesicle or V-SNAREs which are found associated with vesicle membranes and target or T-SNAREs which are usually found in target membranes. There are three different types of coat proteins: Clathrin, Coat protein complex (COP) I and II (Pizarro and Norambuena, 2014). COPI is involved in regulating cargo containing vesicles from Golgi to ER and intra-Golgi trafficking while COP II involved in formation of vesicles at ER-golgi complex (Szul and Sztul, 2011). Like COPI and COPII, clathrin plays an important role in formation of coated vesicles and performs critical roles in shaping rounded vesicles in cytoplasm for intracellular trafficking.

The endomembrane trafficking of proteins is regulated via molecular transport involving protein mobilization into vesicles. The ADP-ribosylation factor (ARFs) are a group of Guanine nucleotide binding proteins (G proteins) which act as molecular switches inside cells and are crucial for endomembrane trafficking of vesicles (Bonifacino and Traub, 2003). G proteins regulate vesicular traffic and organelle structure by recruiting coat proteins, regulating phospholipid metabolism and modulating the structure of actin at membrane surfaces (Bonifacino and Glick,

2004). ARF proteins function through a cycle of GTP binding and GTP hydrolysis, which leads to the GTP-bound active form and the GDP-bound inactive form of the protein (Jackson and Casanova, 2000). This cycle is regulated by guanine nucleotide exchange factors (GEFs) and GTPase-activating proteins (GAPs) (Donaldson and Jackson, 2011). ADP ribosylation factor-guanine nucleotide exchange factors (ARF-GEFs) and ADP ribosylation factor-GTPase activating proteins (ARF-GAPs) therefore act in ARF regulation (Donaldson and Jackson, 2011). The rate of nucleotide exchange between GDP and GTP of ARFs is slow when ARFs act alone but can be enhanced by ARF-GEFs that mediate the formation of ARF-GTP, and by ARF-GAPs which mediate the hydrolysis to ARF-GDP (Goldberg, 1998). Among the different factors that control vesicle trafficking, ARF-GEFs and ARF-GAPs have been implicated most strongly in PIN localization during leaf vein patterning (Sieburth et al., 2006; Geldner et al., 2003).

1.8.3 ARF-GEFs in PIN localization

ARF-GEFs contribute to endomembrane trafficking and are involved in secretion, endocytosis and recycling of different proteins (Singh et al., 2018). *Arabidopsis* has eight ARF-GEFs including GNOM and its two homologs GNOM LIKE 1 (GNL1) and GNOM LIKE 2 (GNL2) and also the BIG (BREFELDIN A INHIBITED ARF GUANINE EXCHANGE FACTOR) subfamily that comprises five members BIG1-5 (Geldner et al., 2003). ARF–GEFs contain a Sec7 domain consisting of approximately 200 amino acid residues that can activate ARF proteins (Cox et al., 2004). Brefeldin A (BFA) is a fungal toxin that inhibits vesicular trafficking in eukaryotes by inhibiting the Sec7 domain of certain ARF-GEFs (Jackson and Casanova, 2000). Richter et al found that BIG1-4 proteins control cell membrane dynamics in *Arabidopsis* by regulating vesicle trafficking (Richter et al., 2014). PIN1 is normally localized to the PM, but upon BFA treatment, basally localized PIN1 accumulates in intracellular compartments, the core of which accumulate

PM and endosomal markers which partially overlap with trans-Golgi markers (Geldner et al., 2003)**.** This evidence led to the suggestion that GNOM is required for PIN1 localization to the basal PM by regulating endocytosis and recycling pathways (Geldner et al., 2003). More recently, it has been found that GNOM predominantly localizes to Golgi apparatus suggesting an indirect role for GNOM in maintaining TGN function and recycling of PIN and other proteins to the PM (Naramoto et al., 2014). It has also been found that mutation in *GNOM* results in shorter primary root growth, fewer lateral roots and disturbed in gravitropism response (Geldner et al., 2003a). Additionally, long time application of BFA results in redistribution of internalized PIN1 to the apical localization in the absence of GNOM function. This result suggests that GNOM is primarily working in basal PIN1 localization, whereas BFA resistant ARF-GEFs (GNL1, BIG3 and BIG5) may be involved in apical PIN1 localization (Geldner et al., 2003a).

1.8.4 ARF-GAP in PIN localization

ARF-GAPs activate GTP hydrolysis of ARF proteins, triggering vesicle coat dissociation and allowing for fusion with target membranes (Gebbie et al., 2005). SCARFACE (SFC) is one of the ARF-GAPs which stimulate GTP hydrolysis on yeast ARF1 (Koizumi et al., 2005).

Scarface *(FKD2/VAN3)*

SCARFACE (SFC)/ VASCULAR NETWORK DEFECTIVE 3 (*VAN3)* is a gene that is required for the normal continuous vein pattern formation in leaves and cotyledons, since *sfc/van3/fkd2* mutants produce fragmented vascular tissue and vascular islands (Koizumi et al., 2000; Deyholos et al., 2000; Steynen and Schultz, 2003). The gene has 3 names: *VASCULAR NETWORK DEFECTIVE 3* (*VAN3*) (Koizumi et al., 2000), *SCARFACE* (*SFC*) (Sieburth et al., 2006) and *FORKED2* (*FKD2*) (Steynen and Schultz, 2003). The *VAN3/SFC/FKD2* gene was found to encode an ARF-GAP (Koizumi et al., 2005; Sieburth et al., 2006) with BAR, PH and ankyrin

domains; double mutant analysis suggests that SFC may act in opposition to GNOM (ARF-GEF) (Sieburth et al., 2006). Analysis of truncated versions of SFC linked to Green fluorescent protein (GFP) showed that BAR and PH domains are minimal requirements for subcellular localization of SFC to the TGN (Naramoto et al., 2009). The localization of SFC/VAN3 is reliant on its pleckstrin homology (PH) domain that binds with high affinity to phosphatidylinositol-4 monophosphate PI (4)P (Koizumi et al., 2005). Strong activation of SFC ARF-GAP activity by PI4P, weak stimulation by PI(4,5)P2 and phosphatidic acid (PA), as well as the compromised activity in the absence of the PH domain even with PI(4)P, indicates that the affinity of the PH domain for a specific phospholipid (likely PI4P) is important for the ARF-GAP activity (Naramoto et al., 2009). The *cvl1/cvp2* mutant shows a similar venation phenotype to *sfc/van3* mutants (Naramoto et al., 2009; F. Carland and Nelson, 2009). In absence of *CVPL1* and *CVP2*, SFC protein is mis-localized; compared to its wild type localization in endomembrane vesicles, it is instead in the cytosol (Naramoto et al., 2009). Thus, both phenotypes (*cvp2cvl1* and *sfc*) seem to result from loss of SFC/VAN3 function.

1.8.5 *FORKED1-LIKE (FL)* gene group 1 family

Like *SFC/VAN3*, *CVP2* and *CVL1*, the *FORKED1 (FKD1)* gene is important for formation of a closed vein pattern in *Arabidopsis*, since mutation of *FKD1* results in an open vein pattern with non-meeting veinlets in cotyledon and leaves (Steynen and Schultz, 2003). FKD1 contains a Domain of Unknown Function828 (DUF828) and a plant Pleckstrin homology-like (PH_2) domain (Hou et al., 2010). It has been suggested that FKD1 is a component of an autoregulatory loop that enables auxin canalization by recruitment of PIN1 to the cell membrane (Hou et al.,2010). Using the yeast two-hybrid system, Naramoto in 2009 identified FKD1, which they called VAB (VAN3 binding protein) as interacting with SFC/VAN3. Further, they determined that, in protoplasts,

FKD1/VAB forms a complex with VAN3 that is associated with the PtdIns(4)*P*-enriched membrane domain of the TGN. Strong co-localization of FKD1 and SFC was also found in cotyledon epidermal cells, with all FKD1–GFP-labeled punctae also labeled by SFC–YFP (Mariyamma et al., 2017). These results indicate that a FKD1/SFC complex interacts with membrane localized PI4P through the SFC PH domain or the FKD1 Pleckstrin Homology_2 (PH_2) domain (Naramoto et al., 2009). Consistent with this idea, it has been found that, in the *cvp2cvl1* double mutant, FKD1-GFP, like SFC, is primarily cytosolic (Mariyamma et al., 2017). The FKD1/SFC complex is localized within a RABA-positive sub-compartment of the TGN that is required for transport from the TGN to the plasma membrane (Mariyamma et al., 2017). Based on these data, we can propose that FKD1 and SFC likely act together in the secretory pathway to traffic PIN1 to the plasma membrane via phosphoinositides (Mariyamma et al., 2017).

Based on the similarity of eight other genes to the *FKD1* gene (Hou et al.,2010), the eight genes were named the *FORKED1-LIKE (FL)* family (*FL1-FL8*). All the *FL* genes encode proteins with DUF828 and PH or PL domains. Phylogenetic analysis places the nine *FL* genes including *FKD1* into three groups (Group 1, 2 and 3). Group 1 includes *FKD1* and three closely related genes *FL1*, *FL2* and *FL3*; Group 2 includes *FL4* and *FL8;* Group 3 includes *FL5*, *FL6* and *FL7* (Mariyamma et al., 2018). The severity of the *fkd1* open vein pattern phenotype increased when combined with mutations in other members of the group 1 FL gene family, but not when combined with mutations in Group 3 genes (Mariyamma et al., 2018). PIN1 localization in pro-vascular cells is more symmetric in the Group 1 triple mutant *fkd1/fl2/fl3* indicating that these genes act redundantly to control vein meeting by localizing PIN1 to the proper position (Mariyamma et al., 2018). The *fkd1/fl2/fl3* and *fkd1/fl1-2/fl2/fl3* mutants also show leaf epidermal cell polarity defects that result in leaf deformities such as buckling. The leaf phenotype of the *fkd1/fl2/fl3* and *fkd1/fl1-*

2/fl2/fl3 mutants supports the role of the FL gene family in cell polarity perhaps due to the reduction in the polar localization of PIN in several developmental stages.

1.9 PIN protein phosphorylation and localization

Multiple kinases have been reported to phosphorylate PIN proteins, including PINOID and D6 PROTEIN KINASE (D6PK) which work together with other protein kinases of cAMP-dependent kinase, cGMP-dependent kinase, phospholipid-dependent protein kinase C (AGCVIII) family (Weller et al., 2017). Phosphorylated PIN proteins can be dephosphorylated by Protein Phosphatase 2A (PP2A), Protein Phosphatase 1 (PP1) and PP6 (Karampelias et al., 2016). The AGC, serine/ threonine protein kinases (PINOID, WAG1 and WAG2) and protein phosphatase, PP2A act at the PM (Gao et al., 2008; Michniewicz et al., 2007) to antagonistically regulate PIN proteins through reversible phosphorylation within the hydrophilic loop (HL) (Dhonukshe et al., 2007). It has been found that 3-phosphoinositide-dependent protein kinase1 (PDK1) is a conserved master regulator of AGC kinases in eukaryotic organisms and also regulates polar auxin transport by activating AGC1 clade kinases, resulting in PIN phosphorylation (Xiao and Offringa, 2020).

1.9.1 *PINOID kinase gene*

PID is a member of AGC kinase family that encodes a serine-theronine protein kinase that is responsible for phosphorylation of PIN proteins and thereby affects polar positioning of PIN proteins (Benjamins, Quint, Weijers, Hooykaas, and Offringa, 2001). Over-expression of *PID (*e.g. *35S:PID)* resulted in hyper-phosphorylation of PIN and caused a more apical shift of PIN1 resulting in auxin depletion from roots and collapse of roots. By contrast, PID loss of function resulted in a basal shift in PIN2 polarity resulting in shoot and embryogenesis defects (Friml et al., 2004).

1.9.2 *Rotundas 3 (RON 3-2)*

Protein phosphatase (PP2A) acts on PIN phosphorylation by removing phosphates from PIN family proteins, which is required for targeting of PIN to the basal membrane (Zhang et al., 2010; Friml et al., 2004). It has been found that a phosphatase activity is required for apical-basal localization of PIN proteins and mediating auxin transport-dependent development in *Arabidopsis* (Michniewicz et al., 2007). The RON3 protein positively regulates phosphatase activity during PIN recycling (Karampelias et al., 2016). The phenotype of *ron3-2* includes reduced apical dominance, shovel shaped leaves, reduced lateral root emergence, decreased auxin maximum in the root apical meristem and increased IAA levels in the shoot apex (Karampelias et al., 2016).

Long term objective

The long-term goal of this research is to establish the relationship between localization of different proteins and cell polarity defects in different tissues. Preliminary data (Yu, Van Essen, Reiter and Schultz, unpublished) indicates that all of *cvp2cvl1, sfc, fkd1/fl1-2/fl2/fl3, 35SPID* and *ron3-2* plants have cell polarity defects in roots and leaf epidermis. We hypothesize that the defects to PIN localization in these mutants result in the altered cell polarity. As a first step towards testing this hypothesis, I will introduce a set of fusion proteins (PIN1-GFP, PIN1-RFP, PIN2-GFP, SFC-YFP, FKD1-GFP and SEC-RFP) into these lines. Future assessment of localization of these fusion proteins within different tissue types will allow determination of i) defects to auxin transport in different tissues and cell types (PIN1-GFP, PIN1-RFP, PIN2-GFP); ii) defects to secretory vesicle dynamics (SFC-YFP, FKD1-GFP); iii) defects to the general secretory pathway (SEC-RFP).

Objectives:

1. Introduce a set of fusion proteins (PIN1-GFP, PIN1-RFP, PIN2-GFP, SFC-YFP, FKD1-GFP and SEC-RFP) into *cvp2cvl1, sfc*, *fkd1/fl1-2/fl2/fl3, 35SPID* and *ron3-2* lines.
2. To determine applicability of these lines to future research, conduct a preliminary qualitative analysis of fusion protein localization in selected tissues of mutant lines.

Chapter 2: Materials and Methodology

2.1 Seeds and lines generated

The seeds of five different genotypes, *cvp2/cvl1* (Carland and Nelson, 2009), *fkd1/fl1-2/fl2/fl3* (Prabhakaran Mariyamma et al., 2018), *sfc* (Deyholos, Cordner, Beebe, & Sieburth, 2000), *ron3-2* (Karampelias et al., 2016) and *35S:PID* were obtained from different sources. The *35S:PID* seed line was obtained from Dr. Joanne Chory at The Salk Institute for Biological Studies, USA. *ron3-2* seeds originated from Dr. Mieke Van Lijsebettens at Ghent University, Belgium. *cvp2/cvl1* and *sfc-40* seeds were from Dr. Francine Carland, Yale University, USA. Generation of *fkd1/fl1-2/fl2/fl3* (Prabhakaran Mariyamma et al., 2018) was previously described. *Arabidopsis thaliana*, Columbia (Col-O) ecotype, obtained from Dr. George Haughn from the University of British Columbia, was used as a wild type (WT) control in all experiments.

Crossing was done using genotypes *cvp2/cvl1, fkd1/fl1-2/fl2/fl3, sfc, ron3-2, 35S:PID* as the female parent and lines expressing the corresponding marker proteins, SEC-RFP (Faso et al., 2009), PIN1-GFP (Benková et al., 2003), PIN2-GFP (Xu & Scheres, 2005), PIN1-RFP (Richter et al., 2014), SFC-YFP (Prabhakaran Mariyamma et al., 2018) and FKD1-GFP (Hou et al., 2010) as the male parent. Crossing was done wearing a magnifier for better focus on the stigma. A half-opened flower was chosen and emasculated by carefully removing anthers around the stigma. Similarly, a fully opened flower was selected from which anthers containing pollen were plucked and rubbed 3 to 4 times on the stigma of the female flower. The pollinated stigma was carefully wrapped with saran wrap to avoid subsequent cross pollination. Successful pollination was indicated by the stigma turning purplish brown after 2-3 days and the seed was ready for harvesting within 15-20 days. 30 different F1 genotypes were obtained after crossing. F1 seed was planted,

and plants screened for the wild type or *cvp2/cvl1, fkd1/fl1-2/fl2/fl3, sfc, ron3-2, 35S:PID* phenotype in the F1 generation. In all cases except the dominant *35S:PID*, plants with the recessive phenotype indicated self rather than cross-pollination, therefore only F1 plants with the wild type phenotype were grown further and allowed to self-fertilize to generate the F2 population. As described below, genotypes were screened through F2-F5 generations until lines homozygous for mutant alleles and marker proteins were identified.

2.2 Growth environment of *Arabidopsis thaliana*

Depending on the phenotype to be identified, seed was sown on either soil or *Arabidopsis thaliana* (AT) media**.** The soil potting mixture used for *Arabidopsis thaliana* is 3:1 soil: vermiculite. The soil was thoroughly wetted with deionized water prior to sowing. *Arabidopsis* seeds were sown on AT plates (Ruegger et al., 1998). The concentration of components within AT is as follows: 5 mM KNO_3, 2.5 mM $MgSO_4$, 2.5 mM KH_2PO_4, 2 mM $Ca(NO_3)_2$, 50 mM $C_{10}H_{12}FeN_2O_8$ 0.07 mM H_3BO_3, 0.014 mM $MnCl_2$, 0.0005 mM $CuSO_4.5H_2O$, 0.001 mM $ZnSO_4.7H_2O$, 0.0002 mM $Na_2MoO_4.2H_2O$, 0.001mM NaCl and 0.00001 mM $CaCl_2.6H_2O$. The solution was adjusted to 5.8 pH with 1M KOH, and agar was added to 0.7%. Following sterilization in an autoclave, the autoclaved media was placed in water bath at 55 degrees Celsius for an hour, appropriate antibiotics (see below) were added to the media, followed by aseptically pouring media into sterile Petri plates.

Pots, covered with saran wrap, or covered AT plates were left at 4 degrees Celsius for 3 days for stratification and were then transferred to a growth chamber (AE-60L, Percival Scientific Inc. Boone, Iowa, USA). The day of moving was considered as 0 DAG (Days After Germination). The growth chamber was maintained at 24 degrees Celsius with humidity of 70 percent and

continuous lighting intensity of approximately 130 mmol photons per m^2 per sec obtained from Cool White, Grow Lux and 60W frosted incandescent bulbs (Osram Sylvania Inc, Danvers, USA). After approximately one week, saran wrap was removed from potted plants. Plants remained in growth chambers throughout their entire life cycle before harvesting. Pots were watered at least twice each week to ensure adequate water for plants, especially during the seed maturation period to avoid silique shrinking and seed desiccation.

2.3 Identifying plants with mutation and fusion protein

All fusion proteins except PIN1-GFP are linked to a gene conferring resistance to an antibiotic or herbicide that is lethal to plants, thus resistance can be used as a marker for the fusion protein.

2.3.1 Screening for Hygromycin resistance

The protein markers SEC-RFP, PIN1-RFP and FKD1-GFP are linked to a gene conferring resistance to Hygromycin B via the *bar* gene (Harrison et al., 2006) so they are screened by growing on plates containing 50 μg/ml hygromycin. To make stock solution of hygromycin, 50 mg of Hygromycin B (Hygromycin, GoldBio Catalog # H-270) was dissolved in 1 ml of sterile H20. A 0.22 μm syringe filter was prewetted by drawing through 1ml of sterilized H2O. The Hygromycin stock was then sterilized by being passed through the 0.22 μm syringe filter. The sterilized Hygromycin stock was stored in autoclaved 1.5 ml centrifuge tube and kept in -20 degree Celsius freezer for future use.

2.3.2 Screening for Kanamycin resistance

PIN2-GFP is linked to a kanamycin resistance gene via *npt* II gene (Harrison et al., 2006) , so plants containing PIN2-GFP were identified by survival on AT plates containing kanamycin. To make a

stock solution, 50 mg of Kanamycin Monosulfate (GoldBio Catalog # K-120) was weighed and dissolved in 1000 µl sterilized water. As described for hygromycin, the dissolved kanamycin solution was filter sterilized using a syringe filter into autoclaved microfuge tubes and stored at -20 degrees Celsius.

2.3.3 Screening for Basta resistance

SFC-YFP is linked to the gene *BlpR* encoding resistance for basta so Basta resistance allows selection for lines with SFC-YFP. Glyphosphate (basta) was sprayed on plants at a 1:1000 dilution in water.

Approximately 20-40 seed of each F2 population was sown on selective media (kanamycin or hygromycin) or soil (Basta). To select for kanamycin resistance, indicating the presence of PIN2-GFP, populations segregating for PIN2-GFP were grown on kanamycin containing media, and were screened for kanamycin resistance at 7 DAG. Resistant seedlings were transplanted to soil. Similarly, populations segregating for SEC-RFP, FKD1-GFP, PIN1-RFP were grown on hygromycin containing media and screened for hygromycin resistance at 10DAG after which resistant seedlings were transferred to soil. Finally, populations segregating for SFC-YFP were grown on soil and were sprayed with basta (Glyphosphate) at 12-14 DAG. Only Basta resistant plants survive spraying. In all cases, resistant seedlings were allowed to self-fertilize to produce the next generation, which was again assessed for kanamycin, hygromycin or Basta resistance until a homozygous population was found.

2.3.4 Identifying PIN1-GFP by fluorescence microscopy

Because the PIN1-GFP fusion protein is not associated with resistance to an antibiotic, plants were screened directly for PIN1-GFP expression in roots of the F3 plants after identifying

lines that were homozygous for the mutant leaf phenotype (see below). Populations of plants segregating for PIN1-GFP were grown vertically to reduce disturbance and stress to the root during examination. The roots of 5DAG seedlings were mounted on glass slides and examined under a NIKON E600 fluorescence microscope using a GFP filter. The expression of PIN1-GFP protein was examined in the stele region where PIN1 expression is strongest and compared to a known wild-type line expressing PIN1-GFP.

2.4 Identifying genotype based on phenotype

The leaf phenotype was next assessed in those plants that had been identified as kanamycin, hygromycin or basta resistant in the F2 population. To identify plants homozygous for *fkd1*, *sfc* or *cvp2*, the cotyledon and first leaf were collected at 14DAG and 21 DAG respectively and mounted carefully in Cytoseal60 (Epredia^{TM} 83124) on glass slides. After 24 hours, or whenever the leaves were sufficiently clear to observe the vein pattern, leaves were observed with transmitted light under a Leica dissecting microscope. Plants with a non-meeting cotyledon and leaf vein phenotype were identified as homozygous for the mutation and allowed to self-fertilize, while remaining plants were discarded. Plants homozygous for *ron3-2* were identified by a combination of phenotypic characters including dwarf size, late flowering and leaves that were round, shovel-shaped and had a short petiole. Plants with the dominant *35S:PID* mutation were identified by a combination of phenotypic characters including agravitropic roots, sterile siliques, abnormal bracts (often larger) and multiple siliques coming from the same point on the stem.

2.4.1 DNA extraction

While both the *fkd1/fl1-2/fl2/fl3* quadruple mutant and the *cvp2/cvl1* double mutant have a quantitatively different vein pattern phenotype compared to the *fkd1* and *cvp2* single mutants, the

differences cannot be reliably detected from visual inspection. Thus, genotype was established using molecular markers. In populations segregating for *fkd1, fl1-2, fl2* and *fl3* mutations, the *fkd1* phenotype was screened as described above. DNA extraction was carried out only on plants with the *fkd1* phenotype. DNA was extracted from young leaves using a CTAB DNA extraction protocol (Allen et al., 2006). The recipe for CTAB DNA extraction and nucleic lysis buffers are provided in Appendix I. Immediately prior to use, one volume of CTAB DNA extraction buffer was well mixed with sodium bisulphite (0.3 mg for 10 ml) followed by one volume of Nucleic lysis buffer and 0.4 volume of 5% Sarkosyl. Three to four young leaves (about 100 mg) from an individual plant were placed into a 1.5 ml autoclaved centrifuge tube and kept in liquid nitrogen for a few minutes. Once frozen, the leaves were smoothly ground and crushed with a pestle, after which they were mixed with 300 µl of extraction buffer and then incubated for 1hour in a 65 degrees Celsius water bath. After incubation, 300 µl of chloroform ($CHCl_3$) was added and the sample was centrifuged for 5 minutes. After centrifugation, the supernatant was decanted, without disturbing the protein interface, into a clean, 1.5 ml centrifuge tube. To the supernatant, 200 µl of isopropanol was added, after which it was incubated at 4 degrees Celsius for at least 2 hours. The solution was then centrifuged for 10 minutes, after which the isopropanol was removed. The pellet was washed twice with 70% ethanol and left to air dry for 1-2 hours before being suspended in 40 µl Millipore water.

2.4.2 Polymerase Chain Reaction (PCR) to identify alleles

All of *fl1-2, fl2* and *fl3* are mutant alleles resulting from TDNA insertion, which can be identified by PCR. PCR was done using a combination of forward (left, L) and reverse (right, R) gene-specific primers and also the left border T-DNA primers (Table 1). Homozygous lines with insertions in both chromosomes give a product only with the left border T-DNA and the gene-

specific primer; wild-type plants with no insertions produce a product only with L and R gene-specific primers; heterozygous plants produce a PCR product with both the left border T-DNA and the gene-specific primer and the L and R gene-specific primers. Known wild type DNA and known homozygous mutant DNA were used as templates in control reactions.

PCR:

While preparing master mix of 24 µl for each reaction, 1 mM of well thawed PCR buffer (Mg^{2+} Froggabio buffer), 0.8 mM of dNTPs, 0.4 mM of each forward and reverse primers, 0.28 mM of DMSO and Millipore water was well mixed in 1.5 ml centrifuge tubes. 0.5 µl of FroggaBio *Taq* polymerase was added immediately before adding the solution to PCR tubes with 1 µl of DNA sample. The thermal cycler reaction conditions comprised of initial denaturation at 94 degrees Celsius for five minutes and 15 seconds followed by 35 cycles of 30 seconds denaturation at 94 degrees Celsius, 30 second annealing at 58 degrees Celsius and a minute and fifteen seconds of elongation at 72 degrees Celsius.

Gel Electrophoresis

For electrophoretic gel preparation, 1 % agarose was made by mixing 1 g of agarose with 100 ml of 1x TBE buffer, diluted from 10x TBE buffer. For making 10x TBE buffer, first 54 g of Tris (Trizma Base) and 27.5 g of Boric acid was mixed with approximately 900 ml of RO water. Secondly, 20 ml of 0.5 M EDTA was added into the solution. Final concentration of 10X TBE buffer is 0.089 M Tris base, 0.089 M boric acid and 0.002 M Na2EDTA with pH adjusted to 8. The solution of agarose was microwaved for 1-2 minutes, cooled for 10-15 minutes and poured into gel chamber for solidification. The solidified agarose gel was carefully placed into 1X TBE buffer. 25 µL of each amplified DNA sample was mixed with 5 µL of 6X loading dye and 20 µl was loaded carefully into well. Gel electrophoresis was conducted at 90 volts for 30-40 minutes.

The gel was stained in a dilute Ethidium bromide solution for 15-20 minutes, and PCR amplification products were visualized using a UV light.

2.5 Confocal microscopy and analysis

Homozygous lines for mutant and fusion protein were assessed to see localization of fusion proteins in mutant lines. Confocal imaging and analysis were carried out in root, hypocotyl and cotyledons of 3-5 DAG seedlings for the SEC-RFP protein marker in all genotypes (*cvp2/cvl1, fkd1/fl1/fl2/ fl3, sfc, ron3-2, 35S: PID).* Root tips, approximately one centimeter long, were removed from the seedlings with a sharp razor blade and carefully mounted in distilled water. Similarly, for hypocotyls, the cotyledons were removed with a razor blade, the remainder of the seedling (hypocotyl and root) was mounted in distilled water, and the region of the hypocotyl just above the root was observed. For cotyledons, small sections of the cotyledon were cut precisely with a razor blade and mounted, adaxial surface upwards, in distilled water. Roots, cotyledons and hypocotyl were viewed under the 40x oil-immersion objective using an Olympus Fluoview FV1000 inverted confocal microscope. The SEC-RFP fusion protein was excited with a 588nm wavelength laser and 7 percent laser with 565 HV was used. Apoplast of cotyledon, root and hypocotyl was observed for analyzing SEC-RFP localization. For each genotype with SEC-RFP, a minimum of 10 samples of each tissue were observed and analyzed. Representative pictures were selected for analysis and processing.

Similarly, genotypes expressing FKD1-GFP, PIN1-GFP and PIN2-GFP were assessed for fusion protein localization by excitation with the 488nm laser. For FKD1-GFP, cortical cells within the elongation zone of root tips from 2.5 DAG young seedlings were observed using an inverted 40x (oil immersion) objective lens. The 488nm laser was maintained at 15 percent, HV was maintained at 685 with 7 percent offset. For PIN1-GFP and PIN2-GFP, four DAG seedlings were

observed under confocal microscopy. For PIN1-GFP, cells within the meristematic zone of the stele where PIN1-GFP is most strongly expressed were observed, and the 488nm laser was maintained at 15% with 658 HV. For PIN2-GFP, cells within the meristematic zone of the epidermis were observed, and the laser was maintained 15 percent with HV at 635.

2.5.1 Image analysis: Image J plotting

NIH image J software was used to compare fusion protein localization and intensity between different lines. To compare protein intensity in different regions of the tissue, pixel intensity values along a designated line were generated by the software.

2.5.2 Statistical analysis

Based on the NIH image generated plot graphs, pixel intensity was recorded and both mean value and standard deviation was calculated from six samples. After determining if the data was homoscedastic or heteroscedastic through F-tests, pairwise, two-tailed T-tests were done to assess differences in localization between and within genotypes.

Table 1

Allele name	**Seed line**	**Forward Primer**	**Reverse Primer**
fl1-2	Salk_064024	5’GCTCATTCACCGACAGTCCTCCG3’	5’GGCTGTTGAGATAGACCGTTGTG3’
*fl*2	Salk_026656	5’CACTGCAACAACTACACAGTCC3’	5’CGTGAAGGTCCCTCCTACATGC3’
*fl*3	Salk_013371	5’GTATCACCAAGAACATCTGGTCGC3’	5’CGTGAATCTGAGCGTTATGAGCCCG3’
T-DNA Left border		5’ATTTTGCCGATTTCGGAAC 3’	
*cvl*1	SALK_029945	5’CTTGGTTCTGCAGCAAACG3’	5’CCTCGTTTCTGCTCTATCCG3’

Chapter 3: Results

Generation of lines homozygous for both mutant alleles and marker proteins

After the crossing was done between the genotypes *cvp2/cvl1*, *fkd1/fl1-2/fl2/fl3, sfc*, *ron3-2, 35S:PID* and plants expressing the fusion proteins SEC-RFP, FKD1-GFP, PIN1-GFP, PIN2-GFP, PIN1-RFP and SFC-YFP, the F1 was harvested and was grown on soil. F1 progeny with a wild-type phenotype was allowed to self-fertilize and the resulting F2 was screened for mutant phenotypes and resistance, as indicated in the Methods.

Phenotypic analysis of different mutants

3.1 Hygromycin and Kanamycin resistance

Each line with fusion proteins FKD1-GFP and SEC-RFP, which are resistant to hygromycin (HYG), was screened by growing them on HYG plates. Resistance was analyzed based on root length after 10DAG, where resistant seedlings had long roots and sensitive seedlings had very short roots. In the F2 populations of *cvp2/cvl1, sfc, fkd1/fl1-2/fl2/fl3, 35S:PID* and *ron3-2* segregating with either FKD1-GFP and SEC-RFP, 75 percent of plants were found to be resistant as expected. In the F3, three quarters were found to be resistant and in the F4 and F5, 100 percent of the population was found to be HYG resistant, which showed that the population is homozygous for the fusion protein (Table 2).

For the kanamycin (KAN) resistance associated with PIN2-GFP, roots were analyzed after 7 DAG. Most of the F2 populations of *cvp2/cvl1, sfc, fkd1/fl1-2/fl2/fl3,* and *ron3-2* segregating with PIN2-GFP were found to be seventy-five percent resistant to kanamycin as expected. In F3, three quarters were found to be resistant and in F4 and F5, 100 percent of the population was found to be KAN resistant which showed the population is homozygous for the fusion protein (Table 2).

3.2 Vein pattern defects identify *fkd1, sfc* and *cvp2/cvl1* mutants

For *fkd1/fl1-2/fl2/fl3, sfc* and *cvp2/cvl1* mutants, cotyledons and first leaves were removed and cleared at 14 DAG and 21 DAG respectively, and then scored for the presence of an open vein pattern, indicating the presence of *fkd1, sfc* or *cvp2* alleles. For *cvp2cvl1,* the ratio of single mutants was 3:1 whereas, for *cvp2cvl1* double mutant, the observed ratio was 1:15 (Table 2).

3.3 Detecting PIN1-GFP and PIN2-GFP by fluorescence microscopy

For PIN1-GFP, all mutants line were analyzed under florescence using a GFP filter. For PIN2-GFP, only the line segregating for *35S:PID* and PIN2-GFP was observed, because antibiotic resistance could not be used as a marker for PIN2-GFP since both transgenes are associated with kanamycin resistance. For PIN1-GFP, the stele region of the root was observed, while for PIN2-GFP, the epidermis was observed. The findings suggest that for *cvp2/cvl1, fkd1/fl1-2/fl2/fl3* and *sfc*, in the F2 and F3 generations, since GFP is dominant, the ratio of GFP expression was 3:1**.** In *ron3-2,* in F2 generation expression of GFP was seventy five percent (Table 2). Since *35S:PID* is also associated with KAN resistance, kanamycin resistance could not be used as an indicator of PIN2-GFP, and rather, fluorescence microscopy was used to determine the presence of PIN2-GFP in *35S:PID* lines. Since I was unable to generate a line homozygous for both PIN2-GFP and *35S:PID,* this genotype was excluded from my confocal analysis.

3.4 PCR test results

In populations derived from crosses between the *fkd1/fl1-2/fl2/fl3* quadruple mutant and lines expressing the fusion protein, DNA was extracted from plants that had first been found to have the *fkd1* leaf vein phenotype and PCR was carried out to find plants that also carried the *fl1-2, fl2* and *fl3* alleles. In populations derived from crosses between the *cvp2/cvl1* quadruple mutant and lines expressing the fusion protein, DNA was extracted from plants with the *cvp2* leaf vein

phenotype and PCR was carried out to find plants that also carried the *cvl1* allele. As an example, in the *fkd1/fl1-2/fl2/fl3* by PIN2-GFP F3 population (Figure 7), I found that plants 1, 3 and 4 had *fl1-2*, *fl2* and *fl3* insertions, and of those, only plant 3 was homozygous for all three alleles (Figure 6). Plant 3 was allowed to self, and I confirmed that its progeny was homozygous for all mutations and antibiotic resistant. Similarly, for the *cvp2cvl1* by PIN2-GFP F3 population, I found that plants 2, 4, 6 and 8 were homozygous for both mutant alleles (Figure 7).

3.5 Confocal results

Among the fusion proteins utilized, all of SEC-RFP, PIN1-GFP and PIN2-GFP have strong expression, and PIN1-GFP and PIN2-GFP are both clearly polarized. PIN1-RFP and PIN1-GFP have the same pattern of expression, but PIN1-GFP intensity is greater than PIN1-RFP. In contrast, FKD1-GFP and SFC-YFP are both expressed at low levels and are expressed within vesicles that do not show obvious polarity. For these reasons, confocal analysis was done only on lines with SEC-RFP, PIN1-GFP and PIN2-GFP.

3.5.1 SEC-RFP localization in *cvp2cvl1, fkd1/fl1-2/fl2/fl3, sfc, ron3-2, 35S:PID*

To examine general defects to secretion, expression and localization of SEC-RFP fusion protein were observed in cotyledon (Figure 1), root tip (Figure 2), hypocotyl (Figure 3) in all five genotypes. In wild type, SEC-RFP is strongly expressed and all of the fusion protein appears to be secreted to the apoplast, since fluorescence is entirely outside the cell (Renna et al., 2013). In the root, cotyledon and hypocotyl of all mutant genotypes, localization of SEC-RFP protein also appeared to be entirely within the apoplast (Figures 1, 2 and 3). To test that there was no quantitative difference between intensity of SEC-RFP fluorescence in the apoplast of the different lines, I plotted pixel intensity in ImageJ (Figure 1). Using the pixel intensity measured in the apoplast of a total of forty cells (4 cells in ten different samples), mean and standard deviation were

determined for each genotype. A Student's t-test indicated that there was no significant difference between the intensity of apoplast SEC-RFP fluorescence in wild type and any mutants in cotyledons (Figure 2-1) root tips (Figure 2-2) or hypocotyls (Figure 2-3)

3.5.2 PIN1-GFP localization in *cvp2cvl1, fkd1/fl1-2/fl2/fl3, sfc, ron3-2, 35S:PID*

Based on previous results, PIN1-GFP is localized on basal side (towards the root tip) of root stele cells (Xi et al., 2016). During my confocal analysis, I observed basal localization of PIN1-GFP in the stele of *sfc, 35S:PID, ron3-2, fkd1/fl1-2/fl2/fl3* roots (Figure 4). In contrast, in the stele of *cvp2/cvl1* roots, PIN1-GFP appeared to be localized to the apical side of cells (Figure 4). To assess whether PIN1-GFP was localized more symmetrically in any of the mutant genotypes, pixel intensity on the apical-basal cell faces was compared to that on the lateral faces. Like wild type, all the mutant genotypes had a significantly higher fluorescence intensity on the apical-basal faces compared to the lateral faces (Figure 4-1). Furthermore, *35S:PID* had significantly reduced fluorescence intensity compared to wild type on both apical-basal and lateral faces, while *cvp2cvl1* had significantly reduced fluorescence intensity compared to wild type on the apical-basal face but not the lateral faces.

3.5.3 PIN2-GFP localization in *cvp2cvl1, fkd1/fl1-2/fl2/fl3, sfc, ron3-2, 35S:PID*

In the wild type, it has been found that PIN2-GFP is apically localized in the root epidermal cells (Rigó et al., 2013). Similarly, in the *cvp2cvl1, ron3-2, fkd1/fl1-2/fl2/fl3 and sfc* mutants, localization was also apical and appeared indistinguishable from wild type (Figure 5). After comparing apical-basal and lateral localization, all mutants, like wild type, were found to have significantly more apical-basal than lateral localization. As well, the intensity of PIN2-GFP in the mutants on either apical-basal or lateral sides was not significantly different from that of wild type (Table 5-1).

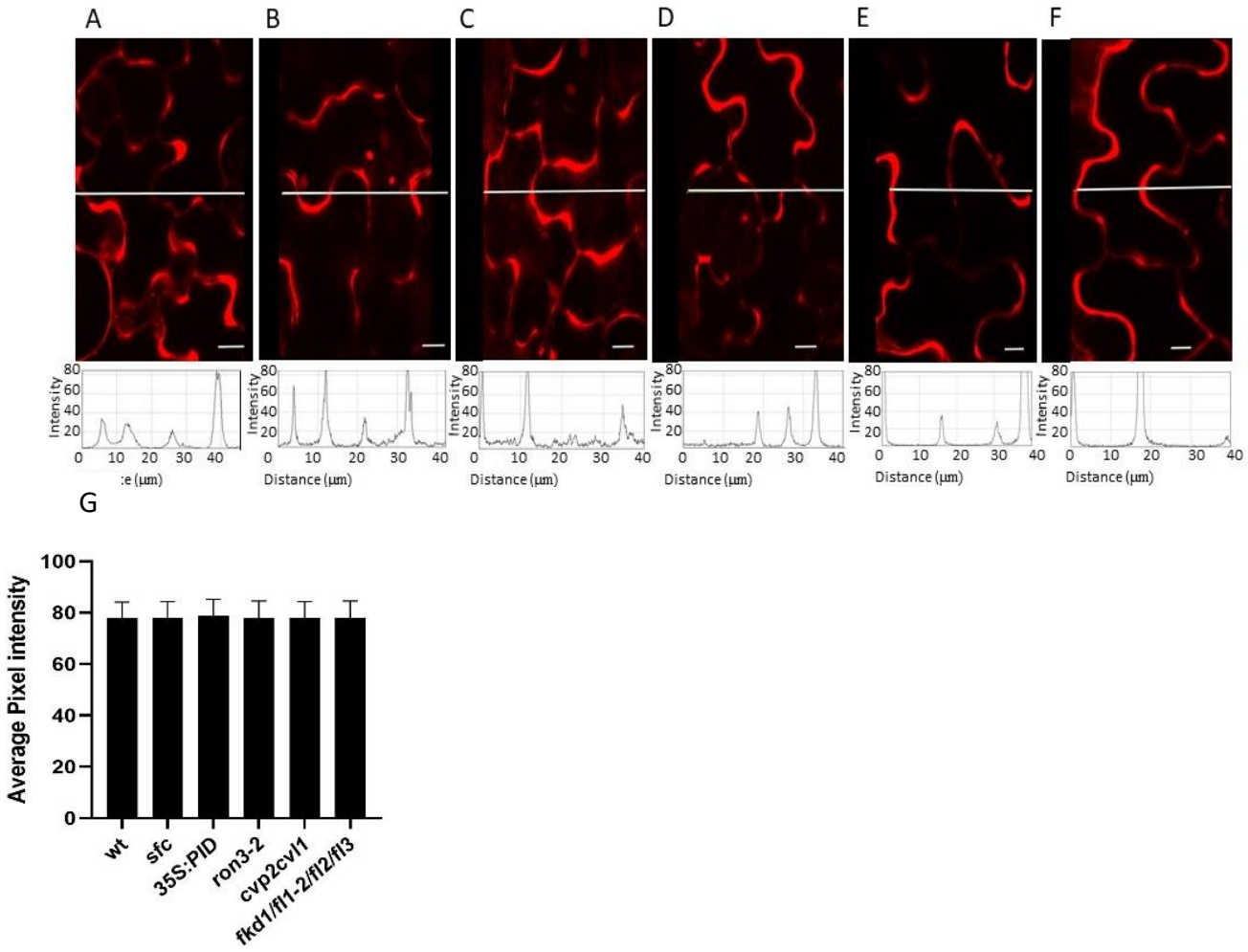

Figure 1: Localization of SEC-RFP proteins in cotyledons of wild type and different mutants: **(A)** WT SEC-RFP; **(B)** *sfc* SEC-RFP; **(C)** *35S:PID* SEC-RFP **(D)** *ron3-2* SEC-RFP **(E)** *cvp2cvl1* SEC-RFP; **(F)** *fkd1/fl1-2/fl2/fl3* SEC-RFP. The pictures are representative images from approximately 10 samples of each genotype. The horizontal white lines in A-F indicate the position at which intensity of RFP emission is measured in the graphs below. The length of scale bar is 40 µm. **(G)** Pixel intensity of SEC-RFP protein within the apoplast of cotyledon epidermal cells of different genotypes. Data are means ± S.D, n= 40 (four cells from each of 10 cotyledons).

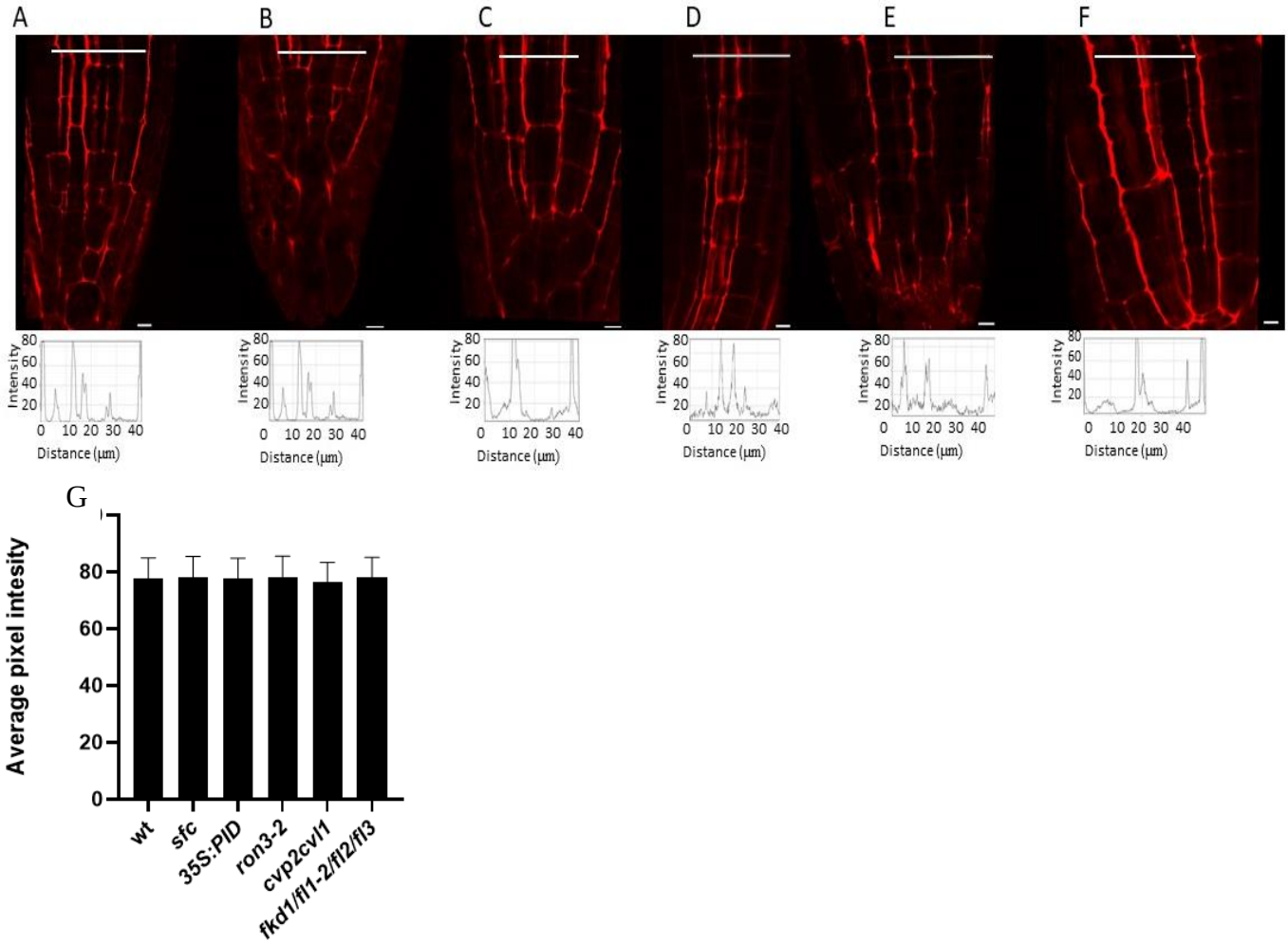

Figure 2: Localization of SEC-RFP proteins in root of wild type and different mutants: **(A)** WT SEC-RFP; **(B)** *sfc* SEC-RFP; **(C)** *35S:PID* SEC-RFP **(D)** *ron3-2* SEC-RFP **(E)** *cvp2cvl1* SEC-RFP; **(F)** *fkd1/fl1-2/fl2/fl3* SEC-RFP. The pictures are representative images from approximately 10 samples of each genotype. The horizontal white lines in A-F indicate the position at which intensity of RFP emission is measured in the plot graphs below. The length of scale bar is 40 µm. **(G)** Pixel intensity of SEC-RFP protein within the apoplast of roots of different genotypes. Data are means ± S.D, n= 40 (four cells from each of 10 roots).

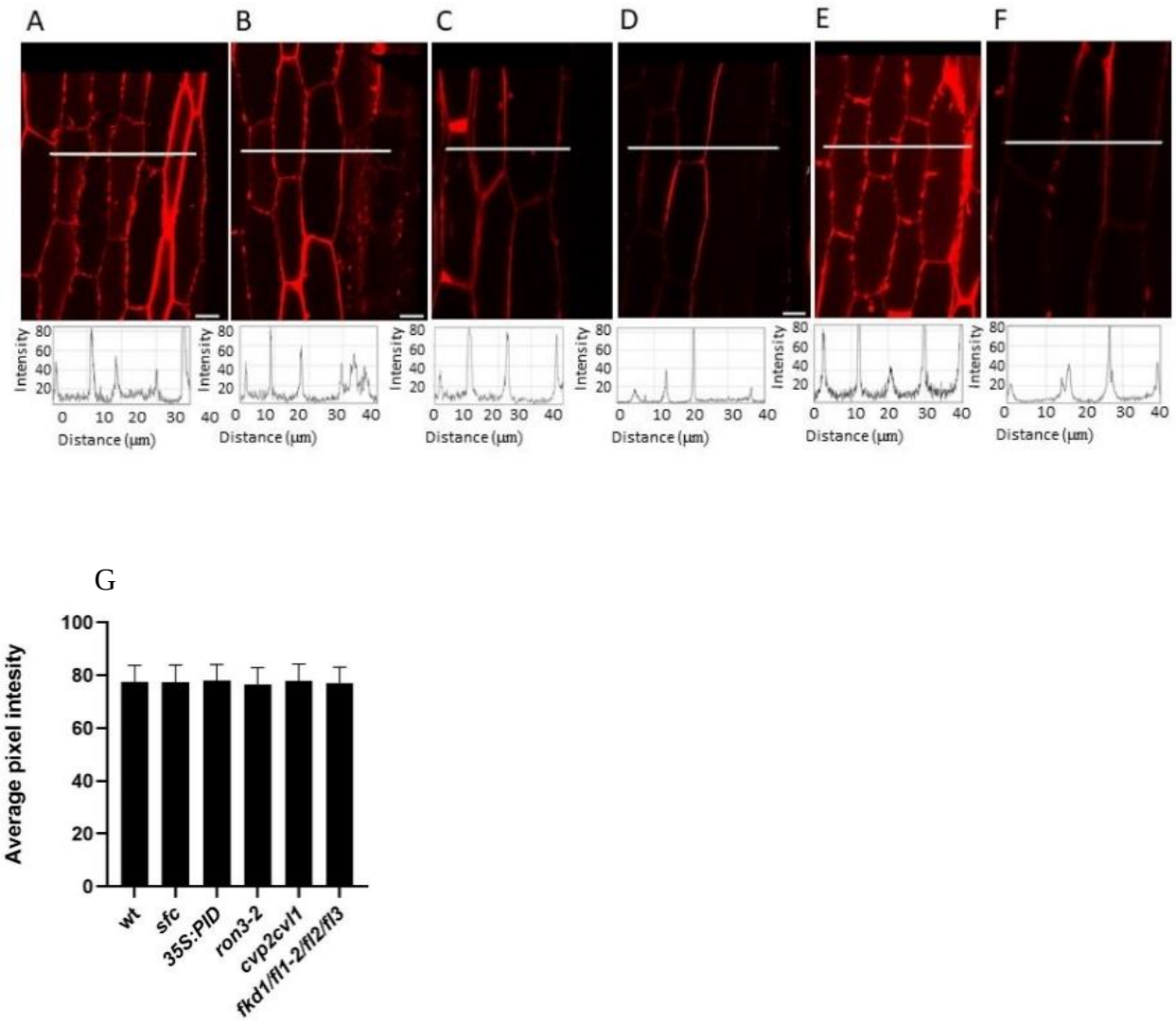

Figure 3: Localization of SEC-RFP proteins in hypocotyl epidermal cells of wild type and different mutants **(A)**WT SEC-RFP; **(B)** *sfc* SEC-RFP; **(C)** *35S:PID* SEC-RFP **(D)** *ron3-2* SEC-RFP **(E)** *cvp2cvl1* SEC-RFP; **(F)** *fkd1/fl1-2/fl2/fl3* SEC-RFP. The plot values were obtained along the white line; the scale bar is 10 µm. All pictures are representative images from approximately 10 samples (n) of each genotype. **(G)** Pixel intensity of SEC-RFP protein within the apoplast of roots of different genotypes. Data are means ± S.D, n= 40 (four cells from each of 10 roots).

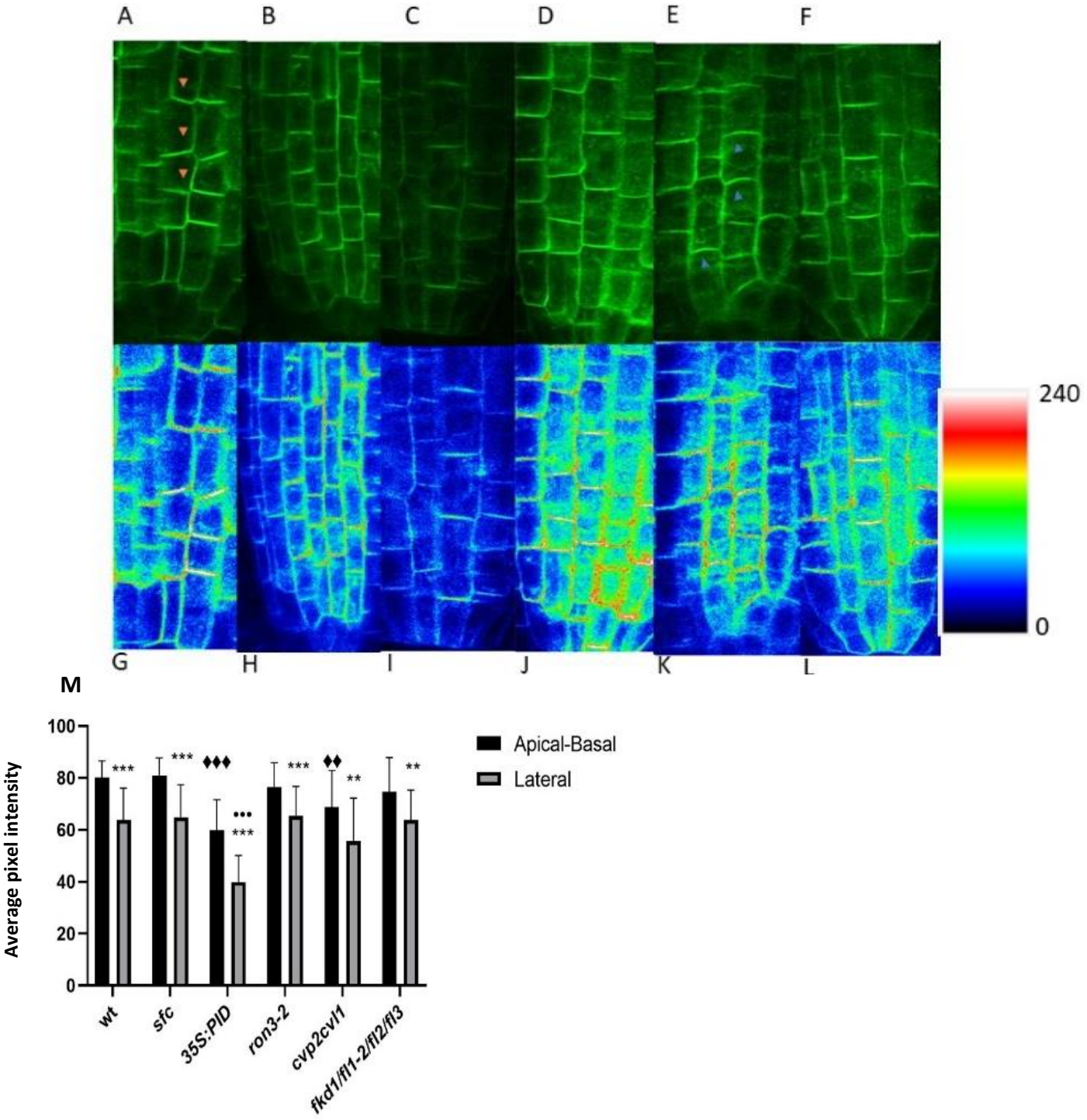

Figure 4: Localization of PIN1-GFP proteins in root of wild type and different mutants **(A-F – GFP indicated by green colour)** WT PIN1-GFP; **(B)** *sfc* PIN1-GFP **(C)** *35S:PID* PIN1-GFP **(D)** *ron3-2* PIN1-GFP; **(E)** *cvp2/cvl1* PIN1-GFP **(F)** *fkd1/fl1-2/fl2/fl3* PIN1-GFP **(G-L intensity**

indicated by colour spectrum on look up table (LUT)**)**; **(G)** WT PIN1-GFP **(H)** *sfc* PIN1-GFP **(I)** *35s:pid* PIN1-GFP **(J)** *ron3-2* PIN1-GFP **(K)** *cvp2/cvl1* PIN1-GFP **(L)** *fkd1/fl1-2/fl2/fl3 PIN1-GFP*. All pictures are a representative image from approximately 10 samples of each genotype. **(M)** Pixel intensity of PIN1-GFP protein in the root stele cells of different genotypes. Data are means ± S.D, n= 40 (four cells from each of 10 roots). The * indicates significant difference between apical-basal and lateral localization intensity within genotypes. The ♦ indicates significant difference of apical-basal localization intensity between wild type and mutant genotype. The • indicates significant difference of lateral localization intensity between wild type and mutant genotype. For all symbols, one (*) indicates $P < 0.05$, two (**) indicates $P < 0.01$ and three (***) indicates $P < 0.001$ based on Students's t-test.

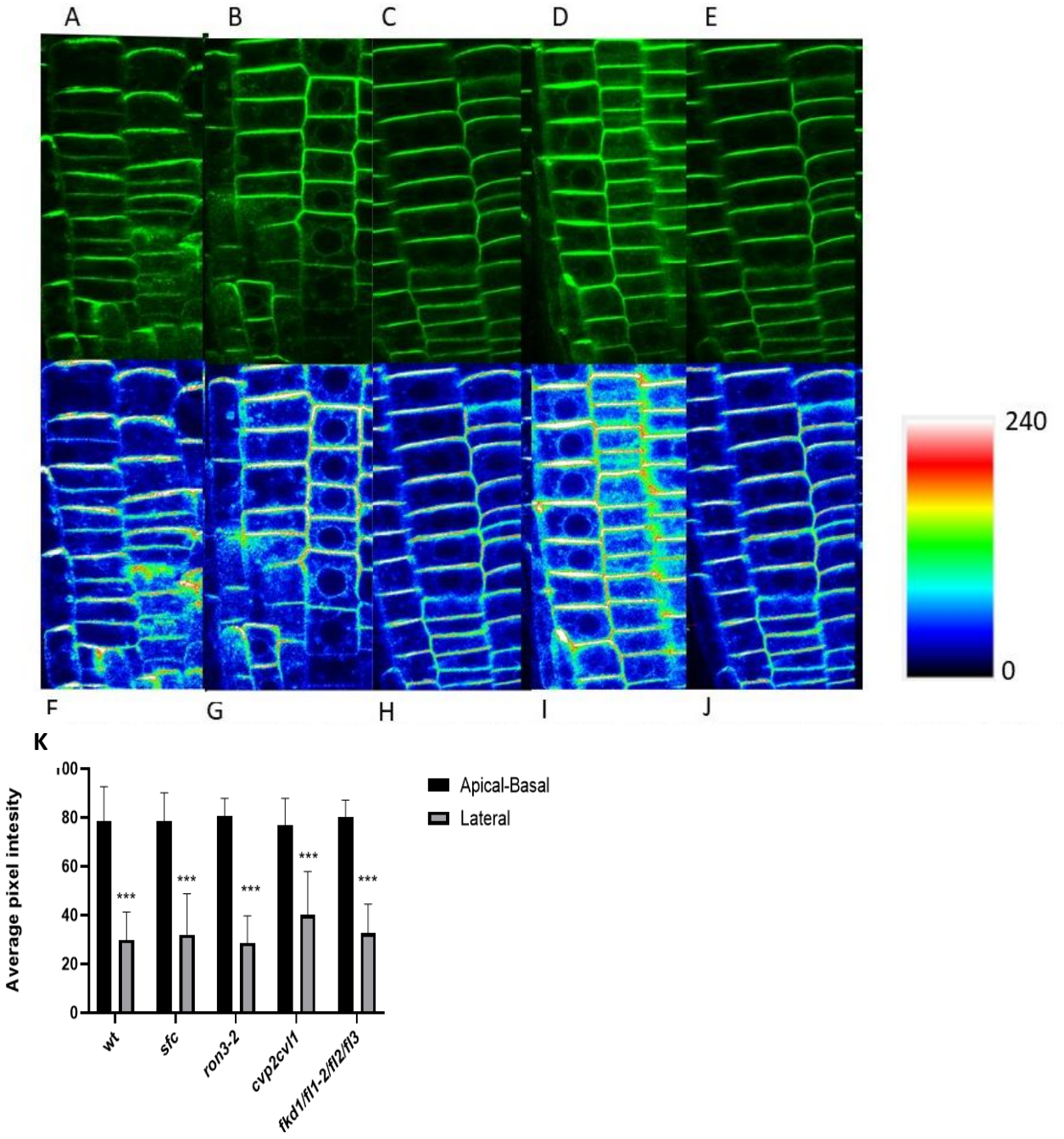

Figure 5: Localization of PIN2-GFP proteins in root epidermal cells of wild type and different mutants **(A-E GFP indicated by green colour) (A)** WT PIN2-GFP **(B)** *sfc* PIN2-GFP **(C)** *ron3-2* PIN2-GFP **(D)** *cvp2/cvl1* PIN2-GFP **(E)** *fkd1/fl1-2/fl2/fl3* PIN2-GFP **((F-L intensity indicated by colour spectrum on** look up table (LUT)**)) (F)** WT PIN2-GFP **(G)** *sfc* PIN2-GFP **(H)** *ron3-2* PIN2-GFP **(I)** *cvp2/cvl1* PIN2-GFP **(J)** *fkd1/fl1-2/fl2/fl3* PIN2-GFP. All pictures are a representative image from approximately 10 samples (n) of each genotype. **(K)** Pixel intensity of PIN2-GFP protein in root epidermal cells of the different genotypes. Data are means ± S.D, n= 40 (four cells from each of 10 roots). The *** indicates significant difference between apical-basal and lateral localization within each genotype based on T-test value ($P < 0.001$). No significant differences

were found when comparing intensity of apical-basal or lateral localization between wild type and mutants.

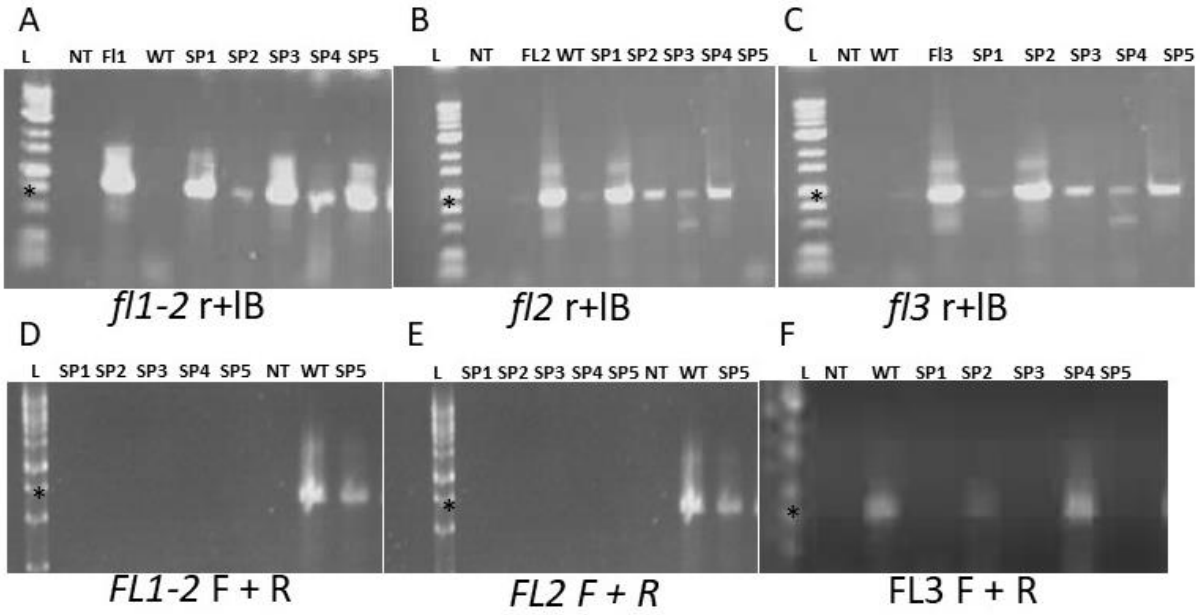

Figure 6: Identifying FL1, FL2 and FL3 alleles within a population of 5 F3 plants from the *fkd1/fl1-2/fl2/fl3* x PIN2-GFP cross using PCR. DNA from wild type (WT, used as a control for the wild type alleles), the *fkd1/fl1-2/fl2/fl3* quadruple mutant (flQ, used as a control for the *fl1-2, fl2, fl3* alleles) and 5 F3 plants from the *fkd1/fl1-2/fl2/fl3* x PIN2-GFP cross (SP1 to SP5) were used as template DNA; RNase water was used as no template (NT) control. The R + lb primers were used to amplify the *fl1-2* (A), *fl2* (B), or *fl3* (C) alleles, and F + R primers were used to amplify the *FL1* (D), *FL2* (E) and *FL3* (F) alleles (see Table 1 for gene specific primers). (**A)** Gel electrophoresis of PCR amplification products from five F3 plants (SP1, SP2, SP3, SP4, SP5) amplified with the R primer specific to the *fl1-2* allele and the LB primer, (**B)** Gel electrophoresis of PCR amplification products from five F3 plants amplified with the R primer specific to the *fl2* allele R and the LB primer, (**C**) Gel electrophoresis of PCR amplification products from five F3 plants tested with *fl3* allele R and LB primer, (**D**) Gel electrophoresis of PCR amplification products from five F3 plants amplified with the F and R primers specific to the *FL1* allele, **(E)** Gel electrophoresis of PCR amplification products from five F3 plants amplified with the F and R primers specific to the *FL2* allele, (**F)** Gel electrophoresis of PCR amplification products from five F3 plants amplified with the F and R primers specific to the *FL3* allele. In all gels, 1Kb ladder (L) was used as a size reference, with 3000 bp fragment indicated (*).

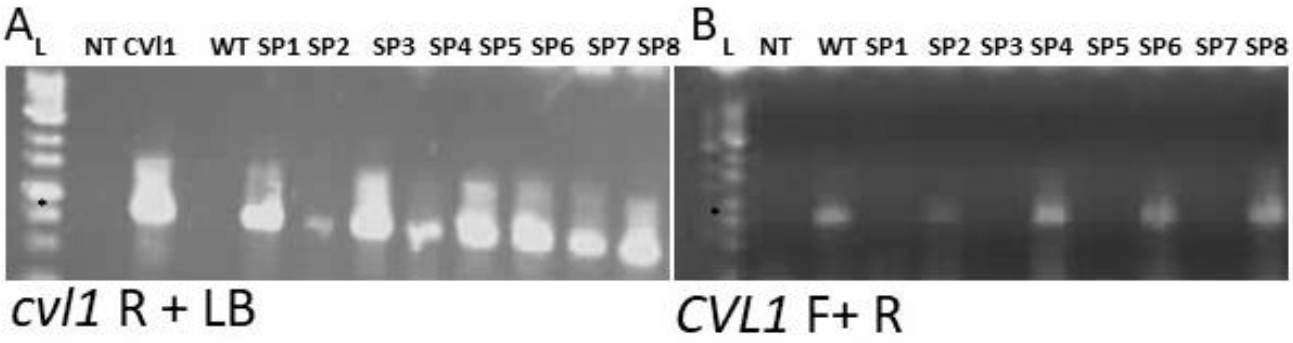

Figure 7: Identifying *CVL1* alleles within a population of 8 F3 plants from the *cvp2cvl1* x PIN2-GFP F3 cross using PCR. PCR reactions were done with template DNA from known *cvp2cvl1* plants (cvl1), wild-type plants (WT) and DNA from plants from the *cvp2cvl1* x PIN2-GFP F3 (SP1 to SP8); RNase water was used as no template (NT) control. A) Gel electrophoresis of PCR amplification products following PCR using *cvl1* R and LB primer. B) Gel electrophoresis of PCR amplification products following PCR using *CVL1* F and R primers. In all gels, 1Kb ladder (L) was used as a size reference, with 3000 bp fragment indicated (*).

Table 2: Frequency of mutant phenotype and fusion protein (via phytotoxin resistance or fluorescence) in successive populations following crossing. Values in bold indicate significantly different from the expected ratio (X^2 test, $P < 0.05$).

Genotypes	**Generation**	**Markers**	**Dominant phenotype**	**Recessive phenotype**	**Chi-square value[a]**	**P value**
sfc * PIN2-GFP	**F2**	KAN[c]	13	7	1.067	0.3017
		sfc[b]	12	8	2.4	0.1213
	F3	KAN[c]	17	3	1.067	0.3017
		sfc[b]	15	5	0.267	0.6059
sfc * PIN1-GFP	**F2**	fluorescence[f]	14	6	0.267	0.6056
		sfc[b]	12	8	2.4	0.1213
	F3	fluorescence[f]	16	4	0.267	0.6056
		sfc[b]	16	4	0.267	0.6056
sfc * FKD1-GFP	**F2**	HYG[c]	16	4	0.267	0.6056
		sfc[b]	13	7	1.067	0.3017
	F3	HYG[c]	18	2	2.4	0.1213
		sfc[b]	16	4	0.267	0.6056
sfc * SEC-RFP	**F2**	HYG[c]	16	6	0.061	0.8055
		sfc[b]	14	8	1.515	0.2184
	F3	HYG[c]	18	2	2.4	0.1213
		sfc[b]	17	3	1.067	0.3017
ron3-2 * PIN2-GFP	**F2**	KAN	14	6	0.267	0.6056
		ron3-2[g]	12	8	2.4	0.1213
	F3	KAN	16	4	0.267	0.6056
		ron3-2[g]	16	4	0.267	0.6056
ron3-2 * PIN1-GFP	**F2**	fluorescence[f]	21	9	0.4	0.5271
		ron3-2[g]	18	12	3.6	0.0578
	F3	fluorescence[f]	25	5	1.111	0.2918
		ron3-2[g]	22	8	0.044	0.833
ron3-2 * FKD1-GFP	**F2**	HYG[c]	20	10	1.111	0.2918
		ron3-2[g]	18	12	3.6	0.0578
	F3	HYG[c]	14	6	0.0267	0.6056
		ron3-2[g]	14	6	0.0267	0.6056
ron3-2 * PIN2-GFP	**F2**	KAN	15	6	0.143	0.7055
		ron3-2[g]	14	7	0.778	0.3778
	F3	KAN	16	4	0.0267	0.6056
		ron3-2[g]	14	6	0.0267	0.6056
35S:PID * PIN1-GFP	**F2**	fluorescence[f]	14	6	0.267	0.6056
		35S:PID[d]	12	8	2.4	0.1213
	F3	fluorescence[f]	16	4	0.267	0.6056
		35S:PID[d]	16	4	0.267	0.6056

35S:PID * FKD1-GFP	**F2**	HYG[c]	14	6	0.267	0.6056
		35S:PID[d]	12	8	2.4	0.1213
	F3	HYG[c]	16	4	0.267	0.6056
		35S:PID[d]	16	4	0.267	0.6056
35S:PID * SEC-RFP	**F2**	HYG[c]	14	6	0.0267	0.6056
		35S:PID[d]	12	8	2.4	0.1213
	F3	HYG[c]	16	4	0.267	0.6056
		35S:PID[d]	16	4	0.267	0.6056
cvp2cvl1 * PIN2-GFP	**F2**	KAN[c]	65	25	0.37	0.5428
		cvp2cvl1 [b,e]	4	65	0.016	0.9003
	F3	KAN[c]	100 percent			
		cvp2cvl1 [b,e]	3	16	2.951	0.0258
cvp2cvl1 * PIN1-GFP	**F2**	fluorescence[f]	20	10	1.111	0.2918
		cvp2cvl1 [b,e]	2	20	0.303	0.5820
	F3	fluorescence[f]	100 percent stained			
		cvp2cvl1 [b,e]	3	14	3.769	0.0522
*cvp2cvl1** SEC-RFP	**F2**	HYG[c]	30	18	**4**	**0.0465**
		cvp2cvl1 [b,e]	3	20	1.812	0.1783
	F3	HYG[c]	14	6	0.267	0.6056
		cvp2cvl1 [b,e]	4	22	3.7	0.0543
flq * SEC-RFP	**F2** HYG		25	35		
	fkd1[b]		10	8	3.630	0.0568
		Homozygous for wt	Heterozygous for mutant	Homozygous for mutants		
	fl1[e]	3	4	3	0.4	0.8187
	fl2[e]	4	2	4	3.6	0.1653
	fl3[e]	3	4	3	0.4	0.8187
flq * SEC-RFP	**F3** HYG					
	fkd1[b]	14	6		0.267	0.6056
		Homozygous for wt	Heterozygous for mutant	Homozygous for mutants		
	fl1[e]	3	8	3	0.286	0.8669
	fl2[e]	2	10	2	2.571	0.2756
	fl3[e]	5	4	5	2.571	0.2765
flq * PIN2-GFP	**F2** KAN					
	fkd1[b]					
		Homozygous for wt	Heterozygous for mutant	Homozygous for mutants		
	fl1[e]	3	5	3	0.091	0.9556
	fl2[e]	4	3	4	2.273	0.3210
	fl3[e]	4	3	4	2.273	0.3210

flq * PIN2-GFP	**F3** KAN					
	fkd1[b]	9	6		1.8	0.1797
		Homozygous for wt	Heterozygous for mutant	Homozygous for mutants		
	fl1[e]	3	3	3	1.0	0.6065
	fl2[e]	4	2	3	3	0.2231
	fl3[e]	4	3	2	1.889	0.3889

[a] the Chi-square value was calculated on the basis of an expected ratio of 3:1 dominant to recessive phenotype for all phenotypes except PCR amplification, where the Chi-square value was calculated on the basis of an expected ratio of 1:2:1 homozygous: heterozygous : homozygous, and the *cvp2cvl1* double mutant, where the Chi-square value was calculated on the basis of an expected ratio 15:1.

[b] screened based on closed (dominant) or open (recessive) vein pattern phenotype

[c] screened based on seedling resistance (dominant) or sensitive (recessive) to 50 ug/ml Hygromycin or Kanamycin

[d] screened based on agravitropic roots, irregular leaf shape (dominant) or gravitropic roots, regular leaf shape (recessive)

[e] mutant and wild type alleles identified via PCR using insertion and gene specific primers (Table 1)

[f] screened based on fluorescence (dominant) or no fluorescence (recessive) under fluorescence microscope

[g] screened based on shovel shaped leaf (dominant), short petiole or normal shaped leaf (recessive)

Chapter 4: Discussion

I have generated thirty different lines by crossing five genotypes, *sfc, 35S:PID, ron3-2, fkd1/fl1-2/fl2/fl3* and *cvp2/cvl1,* with lines expressing 6 different fusion proteins, SEC-RFP, PIN1-GFP, PIN2-GFP, FKD1-GFP, PIN1-RFP and SFC-YFP. Homozygous lines were generated between fusion proteins and mutants through screening for antibiotic (HYG, KAN) resistance, morphological defects and PCR amplification differences. Since PIN1-GFP and PIN1-RFP both have similar pattern of localization, but PIN1-GFP has brighter localization, I chose PIN1-GFP to assess polarity defects. Additionally, FKD1-GFP and SFC-YFP are expressed in low levels and within vesicles that do not show strong polarity. Thus, of the homozygous lines generated, assessment of protein localization and intensity by confocal microscopy was only done for mutants with SEC-RFP, PIN1-GFP, and PIN2-GFP.

SEC-RFP localization was like wild type in all mutant lines.

In all seedlings of all mutant genotypes, I observed SEC-RFP localization in the apoplast of cotyledon, root and hypocotyl. Previous work (Mariyamma et al., 2017) has shown that *fkd1* and *sfc* likely act in the secretory pathway, that the Group 1 FL genes (FL1, FL2 and FL3) act redundantly with FKD1, and that CVP2 and CVL1 activity are required for FKD1 and SFC function. Thus, I hypothesized that these mutants might not only affect PIN protein trafficking, but also the general secretory pathway. If the mutations caused general defects that affected movement of secretory vesicles to the outside of cell, we would expect to observe the SEC-RFP trapped in cytosolic vesicles (Renna et al., 2013) rather than being secreted into the apoplast. My findings from confocal analysis suggest that all SEC-RFP was localized in the apoplast rather than being retained within the cytosol which implied that the secretory pathway was not defective.

PIN1-GFP was basally localized on stele region of mutants and wild type except *cvp2cvl1* and PIN2-GFP was apically localized in the epidermis of all mutants. We hypothesized that the short root phenotype of *cvp2cvl1*, *fkd1/fl1-2/fl2/fl3* might be due to mislocalization of PIN family proteins. It has been found that in *sfc* mutant there is no effect on localization of PIN1-GFP while treating with BFA and after washing BFA or no BFA (Sieburth et al., 2006). As in wild type, PIN1-GFP localization was basal in the stele region of roots in all mutant lines except in *cvp2cvl1*, where PIN1-GFP was found to be apically localized. Whereas overexpression of *PID* has previously been found to induce a basal to apical shift of PIN1-GFP in root stele cells (Huang et al., 2010; Friml et al., 2004 ; Kleine-Vehne et al., 2009), I found no change in PIN1-GFP localization within *35S:PID* mutant lines. As it is unclear why my results differ from the previous findings, this warrants further investigation. As in wild type, PIN2-GFP localization was apical in the epidermal region of roots in all of *sfc*, *ron3-2*, *fkd1/fl1-2/fl2/fl3* and *cvp2/cvl1*. While PIN2-GFP had not been previously assessed in other lines, basal rather than apical localization of PIN2-GFP had been found on root epidermal cells of *ron3-2* mutants (Karampelias et al., 2016).

Future directions

During my Masters program, I have successfully generated thirty different lines after crossing five genotypes. Those lines could be used to study polarity defects on root hairs and leaves vein pattern among different mutants. Though I did confocal analysis only SEC-RFP, PIN1-GFP and PIN2-GFP so far, I have now homozygous lines for all above mentioned mutants which can be assessed in future for further study. Plasmolysis experiments could be done based on my results found on PIN1-GFP localization to find actual location of PIN1 protein on root stele region.

References

Adamowski, M., and Friml, J. (2015). PIN-dependent auxin transport: action, regulation, and evolution. *The Plant Cell, 27*(1), 20-32.

Bayer, E. M., Smith, R. S., Mandel, T., Nakayama, N., Sauer, M., Prusinkiewicz, P., and Kuhlemeier, C. (2009). Integration of transport-based models for phyllotaxis and midvein formation. *Genes and Development, 23*(3), 373-384.

Beemster, G. T., and Baskin, T. I. (1998). Analysis of cell division and elongation underlying the developmental acceleration of root growth in *Arabidopsis thaliana*. *Plant Physiology, 116*(4), 1515-1526.

Benjamins, R., Quint, A., Weijers, D., Hooykaas, P., and Offringa, R. (2001). The PINOID protein kinase regulates organ development in *Arabidopsis* by enhancing polar auxin transport. *Development, 128*(20), 4057-4067.

Benková, E., Michniewicz, M., Sauer, M., Teichmann, T., Seifertová, D., Jürgens, G., and Friml, J. (2003). Local, efflux-dependent auxin gradients as a common module for plant organ formation. *Cell, 115*(5), 591-602.

Bonifacino, J. S., and Glick, B. S. (2004). The mechanisms of vesicle budding and fusion. *Cell, 116*(2), 153-166.

Bonifacino, J. S., and Traub, L. M. (2003). Signals for sorting of transmembrane proteins to endosomes and lysosomes. *Annual Review of Biochemistry, 72*(1), 395-447.

Carland, F., and Nelson, T. (2009). CVP2-and CVL1-mediated phosphoinositide signaling as a regulator of the ARF GAP SFC/VAN3 in establishment of foliar vein patterns. *The Plant Journal, 59*(6), 895-907.

Carland, F. M., and Nelson, T. (2004). COTYLEDON VASCULAR PATTERN2–mediated inositol (1, 4, 5) triphosphate signal transduction is essential for closed venation patterns of *Arabidopsis* foliar organs. *The Plant Cell, 16*(5), 1263-1275.

Celenza, j. J., Grisafi, P. L., and Fink, G. R. (1995). A pathway for lateral root formation in *Arabidopsis thaliana*. *Genes and Development, 9*(17), 2131-2142.

Chandler, J. W. (2009). Local auxin production: a small contribution to a big field. *Bioessays, 31*(1), 60-70.

Cove, D. J. (2000). The generation and modification of cell polarity. *Journal of Experimental Botany, 51*(346), 831-838.

Cox, R., Mason-Gamer, R. J., Jackson, C. L., and Segev, N. (2004). Phylogenetic analysis of Sec7-domain–containing Arf nucleotide exchangers. *Molecular Biology of the Cell, 15*(4), 1487-1505.

De Boer, H. J., Drake, P. L., Wendt, E., Price, C. A., Schulze, E.-D., Turner, N. C., Veneklaas, E. J. (2016). Apparent overinvestment in leaf venation relaxes leaf morphological constraints on photosynthesis in arid habitats. *Plant Physiology, 172*(4), 2286-2299.

De Smet, S., Cuypers, A., Vangronsveld. J., and Remans, T. (2015). Gene networks involved in hormonal control of root developmetn in *Arabidopis thaliana*: A framework for studying its disturbance by metal stress. *International Journal of Molecular Sciences, 16*(8), 19195-19224.

Deyholos, M. K., Cordner, G., Beebe, D., and Sieburth, L. E. (2000). The SCARFACE gene is required for cotyledon and leaf vein patterning. *Development, 127*(15), 3205-3213.

Dhonukshe, P., Aniento, F., Hwang, I., Robinson, D. G., Mravec, J., Stierhof, Y.-D., and Friml, J. (2007). Clathrin-mediated constitutive endocytosis of PIN auxin efflux carriers in *Arabidopsis*. *Current Biology, 17*(6), 520-527.

Dolan, L., Janmaat, K., Willemsen, V., Linstead, P., Poethig, S., Roberts, K., and Scheres, B. (1993). Cellular organisation of the *Arabidopsis thaliana* root. *Development, 119*(1), 71-84.

Donaldson, J. G., and Jackson, C. L. (2011). ARF family G proteins and their regulators: roles in membrane transport, development and disease. *Nature Reviews Molecular cell biology, 12*(6), 362-375.

Drakakaki, G., Van De Ven, W., Pan, S., Miao, Y., Wang, J., Keinath, N. F., Hicks, G. (2012). Isolation and proteomic analysis of the SYP61 compartment reveal its role in exocytic trafficking in *Arabidopsis*. *Cell Research, 22*(2), 413-424.

Du, Y., and Scheres, B. (2018). Lateral root formation and the multiple roles of auxin. *Journal of Experimental Botany, 69*(2), 155-167.

Faso, C., Chen, Y.-N., Tamura, K., Held, M., Zemelis, S., Marti, L., Miller, E. (2009). A missense mutation in the *Arabidopsis* COPII coat protein Sec24A induces the formation of clusters of the endoplasmic reticulum and Golgi apparatus. *The Plant Cell, 21*(11), 3655-3671.

Fischer, U., Ikeda, Y., and Grebe, M. (2007). Planar polarity of root hair positioning in *Arabidopsis*. *Biochemical Society Transactions, 35*(1), 149-151.

Friml, J., Benková, E., Blilou, I., Wisniewska, J., Hamann, T., Ljung, K., Jürgens, G. (2002). AtPIN4 mediates sink-driven auxin gradients and root patterning in *Arabidopsis*. *Cell, 108*(5), 661-673.

Friml, J., Vieten, A., Sauer, M., Weijers, D., Schwarz, H., Hamann, T., Jürgens, G. (2003). Efflux-dependent auxin gradients establish the apical–basal axis of *Arabidopsis*. *Nature, 426*(6963), 147-153.

Friml, J., Yang, X., Michniewicz, M., Weijers, D., Quint, A., Tietz, O., Sandberg, G. (2004). A PINOID-dependent binary switch in apical-basal PIN polar targeting directs auxin efflux. *Science, 306*(5697), 862-865.

Fukuda, H. (2004). Signals that control plant vascular cell differentiation. *Nature Reviews Molecular Cell Biology, 5*(5), 379-391.

Gälweiler, L., Guan, C., Müller, A., Wisman, E., Mendgen, K., Yephremov, A., and Palme, K. (1998). Regulation of polar auxin transport by AtPIN1 in *Arabidopsis* vascular tissue. *Science, 282*(5397), 2226-2230.

Gao, X., Nagawa, S., Wang, G., and Yang, Z. (2008). Cell polarity signaling: focus on polar auxin transport. *Molecular plant, 1*(6), 899-909.

Gebbie, L. K., Burn, J. E., Hocart, C. H., and Williamson, R. E. (2005). Genes encoding ADP-ribosylation factors in *Arabidopsis thaliana* L. Heyn.; genome analysis and antisense suppression. *Journal of Experimental Botany, 56*(414), 1079-1091.

Geldner, N., Anders, N., Wolters, H., Keicher, J., Kornberger, W., Muller, P., . . . Jürgens, G. (2003). The *Arabidopsis* GNOM ARF-GEF mediates endosomal recycling, auxin transport, and auxin-dependent plant growth. *Cell, 112*(2), 219-230.

Goldberg, J. (1998). Structural basis for activation of ARF GTPase: mechanisms of guanine nucleotide exchange and GTP–myristoyl switching. *Cell, 95*(2), 237-248.

Gray, R. S., Roszko, I., and Solnica-Krezel, L. (2011). Planar cell polarity: coordinating morphogenetic cell behaviors with embryonic polarity. *Developmental cell, 21*(1), 120-133.

Grunewald, W., and Friml, J. (2010). The march of the PINs: developmental plasticity by dynamic polar targeting in plant cells. *The EMBO journal, 29*(16), 2700-2714.

Harrison, S. J., Mott, E. K., Parsley, K., Aspinall, S., Gray, J. C., & Cottage, A. (2006). A rapid and robust method of identifying transformed *Arabidopsis thaliana* seedlings following floral dip transformation. *Plant Methods, 2*(1), 1-7.

Heilmann, I. (2016). Phosphoinositide signaling in plant development. *Development, 143*(12), 2044-2055.

Hou, H., Erickson, J., Meservy, J., and Schultz, E. A. (2010). FORKED1 encodes a PH domain protein that is required for PIN1 localization in developing leaf veins. *The Plant Journal, 63*(6), 960-973.

Huang, F., Zago, M. K., Abas, L., van Marion, A., Galván-Ampudia, C. S., & Offringa, R. (2010). Phosphorylation of conserved PIN motifs directs *Arabidopsis* PIN1 polarity and auxin transport. *The Plant Cell, 22*(4), 1129-1142.

Ichihashi, Y., and Tsukaya, H. (2015). Behavior of leaf meristems and their modification. *Frontiers in Plant Science, 6*, 1060-1060.

Ikeda, Y., Men, S., Fischer, U., Stepanova, A. N., Alonso, J. M., Ljung, K., and Grebe, M. (2009). Local auxin biosynthesis modulates gradient-directed planar polarity in *Arabidopsis*. *Nature Cell Biology, 11*(6), 731-738.

Jackson, C. L., and Casanova, J. E. (2000). Turning on ARF: the Sec7 family of guanine-nucleotide-exchange factors. *Trends in Cell Biology, 10*(2), 60-67.

Jürgens, G. (2004). Membrane trafficking in plants. *Annual Review of Cell and Develomental Biology 20*, 481-504.

Karampelias, M., Neyt, P., De Groeve, S., Aesaert, S., Coussens, G., Rolčík, J., . . . Van Montagu, M. (2016). ROTUNDA3 function in plant development by phosphatase 2A-mediated regulation of auxin transporter recycling. *Proceedings of The National Academy of Sciences, 113*(10), 2768-2773.

Keuskamp, D. H., Pollmann, S., Voesenek, L. A., Peeters, A. J., and Pierik, R. (2010). Auxin transport through PIN-FORMED 3 (PIN3) controls shade avoidance and fitness during competition. *Proceedings of the National Academy of Sciences, 107*(52), 22740-22744.

Kleine-Vehn, J., Huang, F., Naramoto, S., Zhang, j., Michniewicz, M., Offringa, R., and Friml, J., (2009). PIN auxin efflux carrier polarity is regulated by PINOID kinase-mediated recruitment into GNOM-independent trafficking in Arabidopsis. *The Plant Cell 21*(12), 3839-3859.

Koizumi, K., Naramoto, S., Sawa, S., Yahara, N., Ueda, T., Nakano, A., . . . Fukuda, H. (2005). VAN3 ARF–GAP-mediated vesicle transport is involved in leaf vascular network formation. *Development, 132*(7), 1699-1711.

Koizumi, K., Sugiyama, M., and Fukuda, H. (2000). A series of novel mutants of *Arabidopsis thaliana* that are defective in the formation of continuous vascular network: calling the auxin signal flow canalization hypothesis into question. *Development, 127*(15), 3197-3204.

Kong, X., Liu, G., Liu, J., and Ding, Z. (2018). The root transition zone: A hot spot for signal crosstalk. *Trends in Plant Science, 23*(5), 403-409.

Kuchen, E. E., Fox, S., De Reuille, P. B., Kennaway, R., Bensmihen, S., Avondo, J., . . . Bangham, A. (2012). Generation of leaf shape through early patterns of growth and tissue polarity. *Science, 335*(6072), 1092-1096.

Łangowski, Ł., Wabnik, K., Li, H., Vanneste, S., Naramoto, S., Tanaka, H., and Friml, J. (2016). Cellular mechanisms for cargo delivery and polarity maintenance at different polar domains in plant cells. *Cell Discovery*, *2*(1), 1-18.

Ljung, K., Bhalerao, R. P., and Sandberg, G. (2001). Sites and homeostatic control of auxin biosynthesis in *Arabidopsis* during vegetative growth. *The Plant Journal*, *28*(4), 465-474.

Ljung, K., Hull, A. K., Celenza, J., Yamada, M., Estelle, M., Normanly, J., and Sandberg, G. (2005). Sites and regulation of auxin biosynthesis in *Arabidopsis* roots. *The Plant Cell*, *17*(4), 1090-1104.

Mashiguchi, K., Tanaka, K., Sakai, T., Sugawara, S., Kawaide, H., Natsume, M., . . . Yao, H. (2011). The main auxin biosynthesis pathway in *Arabidopsis*. *Proceedings of The National Academy of Sciences*, *108*(45), 18512-18517.

Michniewicz, M., Zago, M. K., Abas, L., Weijers, D., Schweighofer, A., Meskiene, I., . . . Huang, F. (2007). Antagonistic regulation of PIN phosphorylation by PP2A and PINOID directs auxin flux. *Cell*, *130*(6), 1044-1056.

Mockaitis, K., and Estelle, M. (2008). Auxin receptors and plant development: a new signaling paradigm. *Annual Review of Cell and Developmental Biology*, *24*, 55-80.

Mravec, J., Skůpa, P., Bailly, A., Hoyerová, K., Křeček, P., Bielach, A., . . . Stierhof, Y.-D. (2009). Subcellular homeostasis of phytohormone auxin is mediated by the ER-localized PIN5 transporter. *Nature*, *459*(7250), 1136-1140.

Naramoto, S., Otegui, M. S., Kutsuna, N., De Rycke, R., Dainobu, T., Karampelias, M., . . . Fukuda, H. (2014). Insights into the localization and function of the membrane trafficking regulator GNOM ARF-GEF at the Golgi apparatus in *Arabidopsis*. *The Plant Cell*, *26*(7), 3062-3076.

Naramoto, S., Sawa, S., Koizumi, K., Uemura, T., Ueda, T., Friml, J., . . . Fukuda, H. (2009). Phosphoinositide-dependent regulation of VAN3 ARF-GAP localization and activity essential for vascular tissue continuity in plants. *Development*, *136*(9), 1529-1538.

Overvoorde, P., Fukaki, H., and Beeckman, T. (2010). Auxin control of root development. *Cold Spring Harbor Perspectives in Biology*, *2*(6), a001537-a001537

Peer, W. A., Blakeslee, J. J., Yang, H., and Murphy, A. S. (2011). Seven things we think we know about auxin transport. *Molecular Plant*, *4*(3), 487-504.

Péret, B., Swarup, K., Ferguson, A., Seth, M., Yang, Y., Dhondt, S., . . . Syed, A. (2012). AUX/LAX genes encode a family of auxin influx transporters that perform distinct functions during *Arabidopsis* development. *The Plant Cell*, *24*(7), 2874-2885.

Petrášek, J., and Friml, J. (2009). Auxin transport routes in plant development. *Development*, *136*(16), 2675-2688.

Petrášek, J., Mravec, J., Bouchard, R., Blakeslee, J. J., Abas, M., Seifertová, D., . . . Čovanová, M. (2006). PIN proteins perform a rate-limiting function in cellular auxin efflux. *Science, 312*(5775), 914-918.

Petricka, J. J., Winter, C. M., and Benfey, P. N. (2012). Control of *Arabidopsis* root development. *Annual Review of Plant Biology, 63*, 563-590.

Pizzaro, L., and Norambuena, L., (2014). Regulation of protein trafficking: Posttranslatonal mechanisms and the unexplored transcirptional control. *Plant Science, 225*, 24-33

Prabhakaran Mariyamma, N., Clarke, K. J., Yu, H., Wilton, E. E., Van Dyk, J., Hou, H., and Schultz, E. A. (2018). Members of the *Arabidopsis* FORKED1-LIKE gene family act to localize PIN1 in developing veins. *Journal of Experimental Botany, 69*(20), 4773-4790.

Prabhakaran Mariyamma, N., Hou, H., Carland, F. M., Nelson, T., and Schultz, E. A. (2017). Localization of *Arabidopsis* FORKED1 to a RABA-positive compartment suggests a role in secretion. *Journal of Experimental Botany, 68*(13), 3375-3390.

Reed, J. W. (2001). Roles and activities of Aux/IAA proteins in *Arabidopsis*. *Trends in Plant Science, 6*(9), 420-425.

Reinhardt, D., Mandel, T., and Kuhlemeier, C. (2000). Auxin regulates the initiation and radial position of plant lateral organs. *The Plant Cell, 12*(4), 507-518.

Reinhardt, D., Pesce, E.-R., Stieger, P., Mandel, T., Baltensperger, K., Bennett, M., Kuhlemeier, C. (2003). Regulation of phyllotaxis by polar auxin transport. *Nature, 426*(6964), 255-260.

Renna, L., Stefano, G., Majeran, W., Micalella, C., Meinnel, T., Giglione, C., & Brandizzi, F. (2013). Golgi traffic and integrity depend on N-myristoyl transferase-1 in *Arabidopsis*. *The Plant Cell, 25*(5), 1756-1773.

Rigó, G., Ayaydin, F., Tietz, O., Zsigmond, L., Kovács, H., Páy, A., Szabados, L. (2013). Inactivation of plasma membrane–localized CDPK-RELATED KINASE5 decelerates PIN2 exocytosis and root gravitropic response in *Arabidopsis*. *The Plant Cell, 25*(5), 1592-1608.

Richter, S., Kientz, M., Brumm, S., Nielsen, M. E., Park, M., Gavidia, R., Mayer, U. (2014). Delivery of endocytosed proteins to the cell–division plane requires change of pathway from recycling to secretion. *Elife, 3*, e02131.

Robert, H. S., and Friml, J. (2009). Auxin and other signals on the move in plants. *Nature Chemical Biology, 5*(5), 325-332.

Rodriguez-Villalon, A., (2015). Wiring a plant: genetic networks for phloem formation in *Arabidopsis thaliana* roots. *New Phytologist, 210* (1), 45-50.

Ruegger, M., Dewey, E., Gray, W. M., Hobbie, L., Turner, J., & Estelle, M. (1998). The TIR1 protein of *Arabidopsis* functions in auxin response and is related to human SKP2 and yeast Grr1p. *Genes & Development, 12*(2), 198-207.

Sack, L., and Scoffoni, C. (2013). Leaf venation: structure, function, development, evolution, ecology and applications in the past, present and future. *New Phytologist, 198*(4), 983-1000.

Sauer, M., Balla, J., Luschnig, C., Wiśniewska, J., Reinöhl, V., Friml, J., and Benková, E. (2006). Canalization of auxin flow by Aux/IAA-ARF-dependent feedback regulation of PIN polarity. *Genes and Development, 20*(20), 2902-2911.

Sawchuk, M. G., and Scarpella, E. (2013). Polarity, continuity, and alignment in plant vascular strands. *Journal of Integrative Plant Biology, 55*(9), 824-834.

Scarpella, E., Marcos, D., Friml, J., and Berleth, T. (2006). Control of leaf vascular patterning by polar auxin transport. *Genes and Development, 20*(8), 1015-1027.

Shao, W., and Dong, J. (2016). Polarity in plant asymmetric cell division: Division orientation and cell fate differentiation. *Developmental Biology, 419*(1), 121-131.

Sieburth, L. E., Muday, G. K., King, E. J., Benton, G., Kim, S., Metcalf, K. E., . . . Van Norman, J. M. (2006). SCARFACE encodes an ARF-GAP that is required for normal auxin efflux and vein patterning in *Arabidopsis*. *The Plant Cell, 18*(6), 1396-1411.

Simon, M. L. A., Platre, M. P., Assil, S., van Wijk, R., Chen, W. Y., Chory, J., . . . Jaillais, Y. (2014). A multi-colour/multi-affinity marker set to visualize phosphoinositide dynamics in A rabidopsis. *The Plant Journal, 77*(2), 322-337.

Singh, M. K., Richter, S., Beckmann, H., Kientz, M., Stierhof, Y.-D., Anders, N., . . . Thomann, A. (2018). A single class of ARF GTPase activated by several pathway-specific ARF-GEFs regulates essential membrane traffic in *Arabidopsis*. *PLoS Genetics, 14*(11), e1007795.

Singh, M., Jadhav, H. R and Bhatt, T. (2017). Dynamin function and ligands: Classical mechanism behin. *Molecular Pharmacology, 91*(2), 123-134.

Steynen, Q. J., and Schultz, E. A. (2003). The FORKED genes are essential for distal vein meeting in *Arabidopsis*. *Development, 130*(19), 4695-4708.

Swarup, R., Kramer, E. M., Perry, P., Knox, K., Leyser, H. O., Haseloff, J., . . . Bennett, M. J. (2005). Root gravitropism requires lateral root cap and epidermal cells for transport and response to a mobile auxin signal. *Nature Cell Biology, 7*(11), 1057-1065.

Swarup, R., and Péret, B. (2012). AUX/LAX family of auxin influx carriers an overview. *Frontiers in Plant Science, 3*, 225-225.

Szul, T., and Sztul, E. (2011). COPII and COPI taffic at the ER-golgi interface. *Physiology (Bethesda, Md.). 26*(5), 348-364.

Tejos, R., Sauer, M., Vanneste, S., Palacios-Gomez, M., Li, H., Heilmann, M., . . . Munnik, T. (2014). Bipolar plasma membrane distribution of phosphoinositides and their requirement for auxin-mediated cell polarity and patterning in *Arabidopsis*. *The Plant Cell, 26*(5), 2114-2128.

Verstraeten, I., Schotte, S., and Geelen, D. (2014). Hypocotyl adventitious root organogenesis differs from lateral root development. *Frontiers in Plant Science, 495*(5), 1-13.

Vieten, A., Vanneste, S., Wiśniewska, J., Benková, E., Benjamins, R., Beeckman, T., . . . Friml, J. (2005). Functional redundancy of PIN proteins is accompanied by auxin-dependent cross-regulation of PIN expression. *Development, 132*(20), 4521-4531.

Viotti, C., Bubeck, J., Stierhof, Y.-D., Krebs, M., Langhans, M., van den Berg, W., . . . Takano, J. (2010). Endocytic and secretory traffic in *Arabidopsis* merge in the trans-Golgi network/early endosome, an independent and highly dynamic organelle. *The Plant Cell, 22*(4), 1344-1357.

Wakelam, M. J., and Lemmon, M. A. (2007). Pleckstrin homology (PH) domains and phosphoinositides. *Biochemical Society Symposia, 74*, 81-93.

Weijers, D., Schlereth, A., Ehrismann, J. S., Schwank, G., Kientz, M., and Jürgens, G. (2006). Auxin triggers transient local signaling for cell specification in *Arabidopsis* embryogenesis. *Developmental Cell, 10*(2), 265-270.

Weller, B., Zourelidou, M., Frank, L., Barbosa, I. C., Fastner, A., Richter, S., Schwechheimer, C. (2017). Dynamic PIN-FORMED auxin efflux carrier phosphorylation at the plasma membrane controls auxin efflux-dependent growth. *Proceedings of the National Academy of Sciences, 114*(5), E887-E896.

Xiao, Y., and Offringa, R. (2020). PDK1 regulates auxin transport and *Arabidopsis* vascular development through AGC1 kinase PAX. *Nature Plants, 6*(5), 544-555.

Xi, W., Gong, X., Yang, Q., Yu, H., & Liou, Y. C (2016). Pin1At regualtes PIN1 polar localization and root graviropism. *Nature Communication, 7*(1), 1-10.

Xu, J., & Scheres, B. (2005). Dissection of *Arabidopsis* ADP-RIBOSYLATION FACTOR 1 function in epidermal cell polarity. *The Plant Cell, 17*(2), 525-536.

Zažímalová, E., Murphy, A. S., Yang, H., Hoyerová, K., and Hošek, P. (2010). Auxin transporters—why so many? *Cold Spring Harbor Perspectives in Biology, 2*(3), a001552-a001552.

Zhang, J., Nodzyński, T., Pěnčík, A., Rolčík, J., and Friml, J. (2010). PIN phosphorylation is sufficient to mediate PIN polarity and direct auxin transport. *Proceedings of the National Academy of Sciences, 107*(2), 918-922.

Zhao, Y. (2012). Auxin biosynthesis: a simple two-step pathway converts tryptophan to indole-3-acetic acid in plants. *Molecular Plant, 5*(2), 334-338.

APPENDIX I

DNA extraction buffer (500 ml)
31.8 g Sorbitol
6 g Trizma
0.84 g EDTA

Add above compounds to 450 ml deionized water. Adjust pH to 7.5 with HCl. Bring to final volume with deionized water.

Nucleic lysis buffer (1000 ml)
200 ml Tris 1M
200 ml EDTA 0.25 M
400 ml NaCl 5M
20g CTAB

Add above solutions to 200 ml deionized water. Add CTAB and heat to dissolve. Adjust pH to 7.5 with HCl. Bring to final volume with deionized water.